Thesis for the Degree of Doctor of Philosophy
in
Thermo and Fluid Dynamics

# Dual-Fuel Combustion in a Heavy-Duty Engine

ZHIQIN JIA

Department of Mechanics and Maritime Sciences
Chalmers University of Technology
Göteborg, Sweden 2018

Dual-Fuel Combustion in a
Heavy-Duty Engine

ZHIQIN JIA

ISBN 978-91-7597-696-9



Doktorsavhandlingar vid Chalmers tekniska högskola
Ny serie nr 4377
ISSN 0346-718X

Department of Mechanics and Maritime Sciences
Chalmers University of Technology
SE–412 96 Göteborg
Sweden
Telephone: +46(0)31- 772 1000

Typeset by the author using LaTeX.

Chalmers Reproservice
Göteborg, Sweden 2018

# Abstract

The need to control climate change and improve the fuel efficiency of internal combustion engines has prompted global efforts to develop alternative fuels in order to reduce dependence on conventional petroleum derivatives. This thesis deals with three such alternative fuels: compressed natural gas (CNG), pure methane (used to mimic biogas), and methanol.

The first parts of the thesis discuss experimental investigations into conventional gas-Diesel dual-fuel combustion. The effect of the CNG/methane supplement ratio on engine performance and emissions was explored at two different load points. The results indicated improved performance and emissions at intermediate load more than at low load. In addition, a 3D dual-fuel combustion model developed at Chalmers was validated against experimental data generated during these studies. Reasonably good agreement was achieved between experiment and simulation for most aspects of engine performance, but there were some discrepancies regarding the onset of ignition delay and emissions.

The later parts of the thesis deal with studies on a low temperature combustion concept, Reactivity Controlled Compression Ignition (RCCI), using two alternative fuels: CNG and methanol. Engine performance and emissions were studied for both CNG-Diesel and methanol-Diesel RCCI combustion. Experiments on CNG-Diesel RCCI combustion were performed to explore the effects of different engine parameters on engine performance and emissions, revealing that high indicated thermal efficiencies (over 50%) could be achieved. However, this combustion strategy presented difficulties when operating at high load and high compression ratios due to the peak in-cylinder pressure limitation. Another CNG-Diesel RCCI combustion study was therefore conducted, focused on extending the operational load range for this combustion strategy and improving combustion phasing by using late inlet valve closing (IVC). This approach increased the maximum load for CNG-Diesel RCCI combustion by 40% compared to the first CNG-Diesel RCCI study. Finally, experiments on methanol-Diesel RCCI combustion showed that port injection of methanol offered better performance than direct injection of methanol during either the intake stroke or the compression stroke in terms of net indicated thermal efficiency and emissions of HC and CO.

Abstract

# List of publications

This thesis is based on work presented in the following papers:

- **Z. Jia**, I. Denbratt, "Effects of Natural Gas Percentage on Performance and Emissions of a Natural Gas/Diesel Dual-Fuel Engine", *ICSAT 2014*, Sweden.
- **Z. Jia**, V. Golovitchev, I. Denbratt, "Validation of a Dual-Fuel Combustion Model for Heavy Duty Diesel Engines", *FISITA 2014 World Automotive Congress*, the Netherlands.
- **Z. Jia**, I. Denbratt, "Experimental Investigation of Natural Gas-Diesel Dual-Fuel RCCI in a Heavy-Duty Engine", *SAE Int. J Engines*, vol. 8, no. 2, pp: 797-807, 2015.
- **Z. Jia**, I. Denbratt, "Effect of Late Inlet Valve Closing on NG-Diesel RCCI Combustion in a Heavy Duty Engine", *COMODIA 2017*, Japan.
- **Z. Jia**, I. Denbratt, "Experimental Investigation into the Combustion Characteristics of a Methanol-Diesel Heavy Duty Engine Operated in RCCI Mode", manuscript submitted to Fuel in December 2017.

# Acknowledgments

First of all, I would like to express my special thanks to my supervisor Prof. Denbratt for giving me the opportunity to work as a PhD student at the combustion division. I really appreciate your guidance, constant encouragement and fruitful discussions regarding my work.

Dr. Golovitchev is acknowledged for helping me with the simulation-related work. Thanks for your patience in explaining so many details about the model.

The financial support provided by the Swedish Energy Agency and the Combustion Engine Research Center (CERC) at Chalmers is also gratefully acknowledged.

My warm thanks go to the former and current research engineers in the lab. Anders Mattsson, Eugenio De Benito, Dr. Gjirja and Dr. Benham are acknowledged for helping me build the test rig. I'm deeply thankful for all your help.

Many thanks to all my colleagues at the combustion division. I really enjoy the easy-going and relaxed atmosphere that you have helped to create here. Thanks also go out to the former and current PhD students in the division - we have had a lot of fun together during our regular after-work events. Thanks to the girls in the division to organize different girl's events and I am pround of being a member of you. All of you made my time in Chalmers very pleasant. Thanks Elenor Norberg, Ulla Lindberg-Thieme and Blagica Smilevska for their kind assistance.

Finally, special and profound thanks to my parents and my brother, for their support and confidence in me.

# Nomenclature

| | |
|---|---|
| **3D** | Three Dimensional |
| **ATDC** | After Top Dead Center |
| **BMEP** | Brake Mean Effective Pressure |
| **BTDC** | Before Top Dead Center |
| **CAD** | Crank Angle Degree |
| **CI** | Compression Ignition |
| **CFD** | Computational Fluid Dynamics |
| **CFM** | Coherent Flame Model |
| **CNG** | Compressed Natural Gas |
| **CO** | Carbon Monoxide |
| **$CO_2$** | Carbon Dioxide |
| **CR** | Compression Ratio |
| **CTC** | Characteristic Time Combustion |
| **DF** | Dual Fuel |
| **DI** | Direct Injection |
| **EBSFC** | Equivalent Brake Specific Fuel Consumption |
| **EGR** | Exhaust Gas Recirculation |
| **FAME** | Fatty Acid Methyl Ester |
| **GDP** | Gross Domestic Product |
| **GHG** | Green House Gas |
| **GVR** | Gas Vehicles Report |
| **HC** | Unburned Hydrocarbons |
| **HCCI** | Homogeneous Charge Compression Ignition |
| **HTHR** | High Temperature Heat Release |
| **HVO** | Hydrotreatment of Vegetable Oils |
| **IDI** | Indirect Injection |
| **IMEP** | Indicated Mean Effective Pressure |
| **ISFC** | Indicated Specific Fuel Consumption |
| **IVC** | Inlet Valve Closing |
| **LTC** | Low Temperature Combustion |
| **LTHR** | Low Temperature Heat Release |

| | |
|---|---|
| **MSP** | Methanol Substitution Percentage |
| **NG** | Natural Gas |
| **NGSP** | Natural Gas Substitution Percentage |
| **NGV** | Natural Gas Vehicle |
| **NGVA** | Natural & Bio Gas Vehicle Association |
| **$NO_x$** | Nitrogen Oxide |
| **NVO** | Negative Valve Overlap |
| **PI** | Pilot Injection |
| **PM** | Particulate Matter |
| **PPC** | Partially Premixed Combustion |
| **PRR** | Pressure rise rate |
| **RCCI** | Reactivity Controlled Compression Ignition |
| **RME** | Rapeseed Methyl Ester |
| **RoHR** | Rate of Heat Release |
| **SI** | Spark Ignition |
| **SOI** | Start of Injection |
| **TDC** | Top Dead Center |

# Contents

# Chapter 1

# Introduction

## 1.1 Motivation

In recent years, the automotive scientific community and vehicle companies have focused considerable research effort on maximizing overall engine efficiency and reducing harmful emissions from internal combustion engines. Various strategies are used for improving engine efficiency in modern vehicles, including intake pressure boosting (using a turbocharger or supercharger), variable valve timing, and direct fuel injection for high-octane fuel engines. In addition, there have been many studies on newer strategies for further improving engine efficiency. Notably, three low temperature combustion (LTC) concepts (HCCI, PPC and RCCI) have been studied extensively, revealing that indicated thermal efficiencies above 50% can be achieved while maintaining low soot and $NO_x$ emissions. Unlike the the other two LTC concepts, RCCI allows the combustion process to be controlled by the fuel's reactivity. By varying the ratio of high-octane fuel to high-cetane fuel, this concept could potentially be used to control autoignition and tune the fuel-air mixture's reactivity.

Global warming, also known as climate change, is primarily due to emissions of greenhouse gases (GHGs). Different countries have set targets for reducing their GHG emissions to avoid the worst impacts of climate change. The EU 2020 regulations include a target of reducing GHG emissions by 20% relative to the level in 1990. By 2050, the EU aims to reduce its GHG emissions by 80% relative to 1990 levels. Data on EU-wide emissions in 2014 indicate that the transportation sector is responsible for roughly 23% of total GHG emissions, and is the main source of air pollution in cities. Moreover, transportation is the only sector whose GHG emissions remain higher than they were in 1990. Road transport is by far the biggest emit-

ter within this sector, accounting for over 70% of its total GHG emissions. Because $CO_2$ is one of the most important GHGs, it has been the main focus of efforts to reduce GHG emissions from the transportation sector. Petroleum-derived fuels (gasoline and Diesel) play central roles in modern transportation, and are the main sources of its $CO_2$ emissions. One way to reduce $CO_2$ emissions is thus to reduce the proportion of petroleum-derived fuels used in the transportation sector. This could be done by partly or completely replacing petroleum-derived fuels with "low-carbon"fuels such as CNG, biogas or a renewable oxygenated alcohol fuel. The EU aims to obtain 20% of its gross final energy consumption from renewable sources by 2020, with the transportation sector accounting for 10% of total renewable energy use. Well-to-wheels (WTW) analyses of various renewable fuels have shown that they can enable dramatic reductions in GHG emissions - for example, the WTW emissions for methanol and ethanol produced from biomass were calculated to be 90% lower than those for conventional fossil fuels [1].

Toxic pollution is a major environmental threat to human health. The main toxic pollutants emitted by vehicles are nitrogen oxides ($NO_x$), particulate matter (PM), hydrocarbons (HC) and carbon monoxide (CO). Consequently, many countries have made their legal limits on emissions of these substances progressively more stringent in recent years. The two most problematic emissions from Diesel engines are $NO_x$ and PM because conventional Diesel engines suffer from a trade-off whereby they cannot simultaneously achieve low emissions of $NO_x$ and PM. However, the LTC concepts discussed above make it possible to avoid this trade-off by producing low emissions of both pollutants. These concepts rely on high rates of cooled EGR to achieve low combustion temperatures, and high rates of fuel and air premixing to limit soot emissions. Alternative fuels such as alcohols have also been used in CI engines to reduce emissions of $NO_x$ and PM [2–4]. Although most LTC combustion concepts produce HC and CO emissions that exceed the levels specified in the Euro VI regulations because of their low combustion temperatures and the presence of premixed fuel in crevices, these pollutants are fairly easy to remove using aftertreatment systems, at least compared to $NO_x$ and PM.

## 1.2 Background

Global energy consumption has increased year on year as a result of population growth and also improvements in GDP. Over the next three decades, world energy consumption is projected to increase by 28%, driven mostly

by rising prosperity in China and India [5]. Figure 1.1 shows how the world energy consumption of different fuels has changed over the years and also the projection up to 2040. Although the market share of liquid fuels such as gasoline, Diesel and biofuels is projected to decrease from 33% in 2015 to 31% in 2040, they are predicted to dominate over other fuels up to 2040. Among them, liquid biofuels have attracted considerable attention due to their renewable status and potential for reducing GHG emissions. Natural gas (NG) consumption is expected to increase by 43% from 2015 to 2040 due to increasing supplies of tight gas, shale gas and coalbed methane at a relatively low price. Renewable fuels such as biogas and electricity are predicted to increase by 78% from 2015 to 2040 as the largest increase in the world energy consumption. The increasing market share of natural gas and renewable fuels reflects global concerns about air pollution caused by conventional fossil fuels, especially greenhouse gas emissions, $NO_x$ emissions, and particulate matter. NG and biomethane as "low-carbon" fuels will likely offer an attractive option for the electric power, industrial and transport sectors in the foreseeable future.

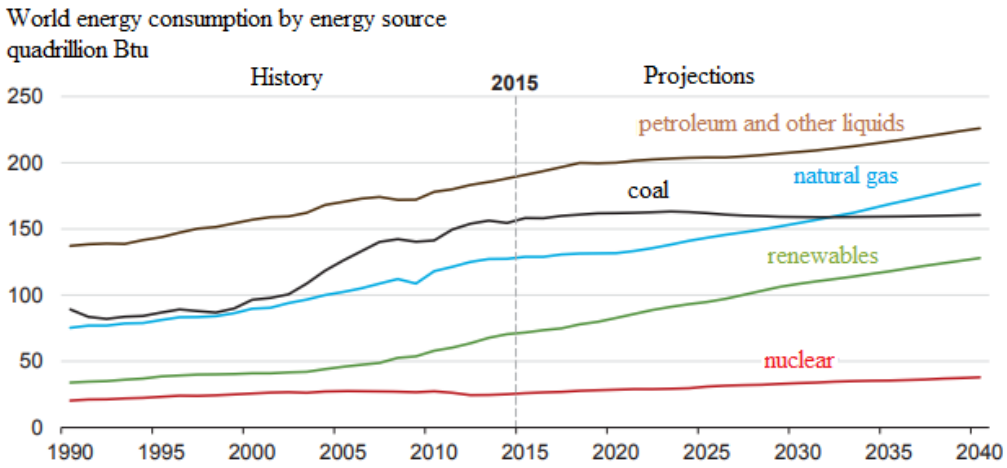


Figure 1.1: Global energy consumption status of different fuels, with projections up to 2040
Source: EIA, International Energy Outlook 2017

Considering the transport sector, the number of natural gas vehicles (NGVs) is increasing rapidly worldwide. The worldwide natural gas vehicle status is shown in Figure 1.2. According to NGVA Europe and the GVR 2013 report, the three largest natural gas vehicle countries are Iran (3.3 million), Pakistan (2.79 million) and Argentina (2.24 million). Together with Brazil, China and India, these six countries have almost 80% of the worldwide existing stock of natural gas vehicles. In contrast, NGVs play a relatively

minor role in Europe. Among the European countries, Italy (0.8 million) has the largest number of NGVs, whereas Sweden only has 44321 NGVs. Most European countries lag behind the global NGV development. Considering the relatively low price of NG and availability of biomethane, gas vehicles may offer a valuable option for Europe in the future.

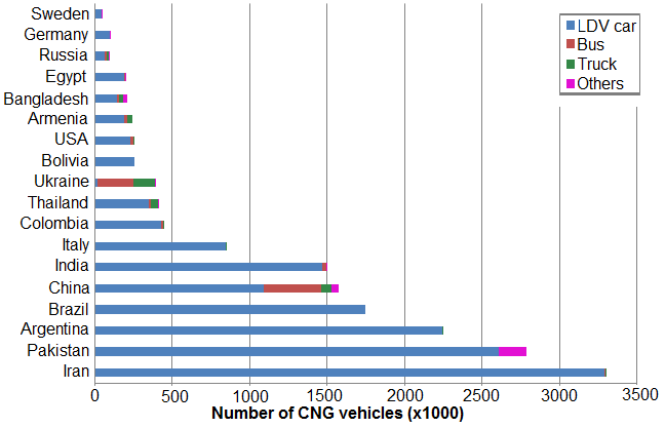


Figure 1.2: Worldwide numbers of natural gas vehicles. LDV=light duty vehicles
Source: NGVA Europe and the GVR (2013).

Owing to the non-renewable characteristic of fossil fuels, global efforts have been devoted to developing renewable energy sources. One important renewable source is biofuels. Figure 1.3 shows worldwide biofuel mandates. Compared with the most stringent countries, such as Brazil and Costa Rico, the EU biofuel mandate is fairly weak. The EU has set mandatory goals of a 20% share for renewable energy in the EU total energy mix by 2020. A minimun 10% out of the 20% share is targeted towards the transportation section for all Member States. The most important biofuel in the EU is bio-Diesel, which accounted for about 70% of the biofuel market on a volume basis in 2012. Traditionally, an esterification process is used to produce Diesel components from vegetable oils. The crops used for biofuel production may potentially be considered to be in competition with food production. Bio-Diesel produced from rapeseed oil is called rapeseed methyl ester (RME). Other acronyms are also used, such as fatty acid methyl ester (FAME). Advanced processes used to produce biofuels include the hydrotreatment of vegetable oils (HVO), anaerobic digestion of organic waste (biogas) and gasification of biomass (biomethane), etc. In Sweden, the biogas market has undergone major development over around 15-20 years. Nowadays, around 44% of the produced biogas is upgraded and fed into the natural gas network to fuel vehicles. The use of biomethane obtained by

gasification of biomass is still in the development stage, and the contribution of this technique is expected to be limited until 2030. Bioalcohols such as biomethanol, bioethanol, biopropanol, and biobutanol are another class of liquid biofuels. They can be produced by fermenting sugar cane, corn, or starches. However, this method of bioalcohol production competes with global food production. Unlike first generation bioalcohols, second generation bioalcohols can be produced from inedible feedstocks sourced from agricultural and forestry wastes, avoiding direct competition with global food product streams.

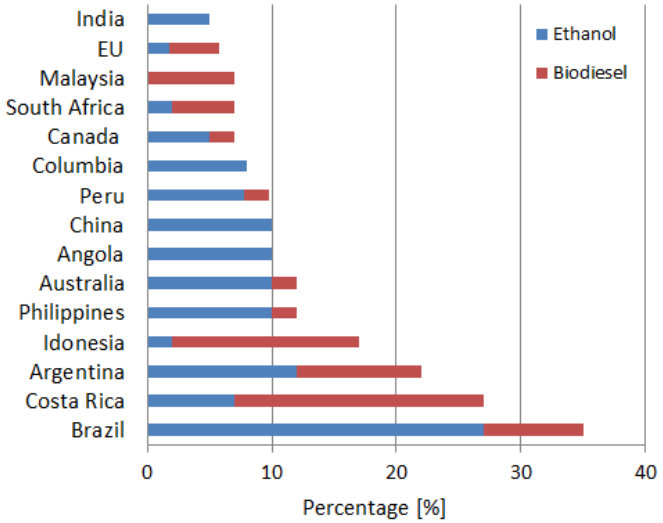


Figure 1.3: Global biofuel mandates. (The data for China were validated only in 9 Provinces. The EU has an overall mandate of only 5.75%, and the separation between ethanol and bio-Diesel was based on the EU Biofuels Annual, 2013 ). Source: Biofuels Digest Biofuels Mandates Around the World 2017

## 1.3 Objectives

The objective of this project was to investigate the dual-fuel combustion in a heavy-duty engine, mainly focused on gaseous fuel (NG and $CH_4$)-Diesel and alcohol fuel (methanol)-Diesel combustion. This thesis involved both conventional dual-fuel combustion and more advanced combustion regime-RCCI combustion. In the first stage of this project, the work was mainly about conventional dual-fuel combustion. In order to investigate the similarities and differences between NG-Diesel and $CH_4$-Diesel conventional dual-fuel combustion, the experiment was performed accordingly by varying the gaseous fuel supplement ratio at two different loads on a Volvo

D12C single cylinder engine. The obtained experimental results were also used to validate a 3D dual-fuel combustion model developed at Chalmers by testing its performance and emissions in cases involving the combustion of pure Diesel, NG-Diesel, and $CH_4$-Diesel. The goal of the first stage work is to understand the combustion similarities and differences between NG-Diesel and $CH_4$-Diesel, and use 3D CFD simulations to clarify details of conventional dual-fuel combustion processes that are not readily characterized experimentally, such as the locations of ignition sites, flame propagation mechanisms, and the formation of specific emissions.

The second stage of the project focused primarily on dual-fuel RCCI combustion: NG-Diesel and methanol-Diesel RCCI combustion, respectively. Three different experimental campaigns were conducted to examine the influence of different parameters. A preliminarily test was conducted to examine the effect of parameters such as SOI, injection quantity, compression ratio, engine speed, and loads on engine performance and emissions of NG-Diesel RCCI combustion. Based on the first study, a second experimental campaign was performed to find ways of extending the operational load range of NG-Diesel RCCI combustion using late inlet valve closing. Additionally, 3D simulation work was conducted to understand NG-Diesel RCCI combustion details using ANSYS FORTE and a chemical mechanism generated using ANSYS Chemkin-Pro. Both of these RCCI test campaigns used port-injected NG, which produces high levels of unburned HC and CO emissions. In an attempt to reduce emissions of these pollutants during dual-fuel RCCI combustion, the plan was to run direct injection of NG and compare with port injection of NG. However, there were some difficulties to run direct injection of NG on time. As an alternative, direct injection of methanol was studied and compared with port injection of methanol. Two different direct methanol injection configurations were studied (direct injection during the intake and compression strokes). The goal of the second stage work is to obtain an in-depth understanding of the dual-fuel RCCI combustion concept, which addresses several issues associated with other premixed compression ignition concepts such as limited combustion phasing control and applicability under high load conditions, as well as, use 3D CFD simulations to clarify details of combustion processes that are not readily characterized experimentally.

# Chapter 2

# Advanced Combustion Strategies

Various low temperature combustion (LTC) concepts such as HCCI, PPC and RCCI have attracted attention in recent years because they could maintain both high engine efficiencies and low emissions of $NO_x$ and soot emissions [6–9].The most common characteristic of LTC concepts is that the fuels are injected at the early phase of intake or compression stroke to allow sufficient time for air-fuel mixing before combustion. This chapter provides an overview of the various LTC concepts.

## 2.1 Homogeneous Charge Compression Ignition (HCCI)

The HCCI strategy relies on the autoignition of a fully premixed air-fuel mixture. One way of realizing HCCI combustion is to use negative valve overlap (NVO) to retain some of the hot residuals in the cylinder, which helps to raise the temperature during the compression stroke, as described by Koopmans et al. [10,11]. HCCI combustion is controlled by chemical kinetics, which makes it difficult to control the combustion phasing and extend the operating region. The operating range for HCCI is limited by combustion stability and combustion efficiency at low load, and by an excessive rate of pressure rise and peak pressure at high load. To extend the low load limit of HCCI, it is necessary to use relatively rich fuel-air mixtures with increased mixture stratification and high in-cylinder temperatures. Various strategies have been developed to achieve these objectives. For example, Koopmans et al. [12] examined the use of a pilot injection into the combustion chamber during the NVO period, and found that the resulting combustion during the gas exchange phase increased the mixture temperature during the main

compression stroke under low load conditions. Chen et al. [13] explored the use of an early inlet valve opening (EIVO) strategy to extend the low load limit by using the residual gas fraction and temperature stratification in the cylinder to maintain stable HCCI combustion. A multiple injection and multiple ignition (MIMI) strategy has also been used to achieve robust HCCI idle operation [14]. The aim of this strategy is to make the mixture ready for autoignition at very light loads by reforming some of the fuel during recompression together with fuel stratification late in the main compression stroke. Other studies have sought to extend the upper load limit of HCCI. Dahl et al. [15–17] achieved fuel stratification by using a late injection during the later part of the compression stroke to reduce pressure fluctuations and thereby extend the upper load limit for HCCI combustion. Additionally, Xu et al. [18] showed that both pressure boosting and EGR are effective at increasing the high load limit of HCCI. However, heavy boosting produced ultra-lean mixtures, which reduced combustion efficiency.

## 2.2 Partially Premixed Combustion (PPC)

PPC is a concept that can be regarded as a combination of the direct injection compression ignition (DICI) and HCCI regimes. It involves a separation between the end of fuel injection and the start of combustion, and uses cooled EGR to reduce $NO_x$ emissions. The longer ignition delay caused by the cooled EGR enables maximal charge premixing, which also reduces soot emissions. To achieve PPC, a high cetane fuel (Diesel) is directly injected in the combustion chamber in the vicinity of top dead center, using a single injection strategy. A large amount of cooled EGR and a low compression ratio are needed to maintain low emissions of $NO_x$ and soot while ensuring the widest possible operating load range [19, 20]. Alriksson and Denbratt [21] examined PPC in a heavy duty single cylinder engine, and achieved similar fuel consumption to conventional Diesel combustion as well as low emissions of $NO_x$ and soot. Fuels with high octane numbers (e.g. gasoline) can also be used in PPC mode. Because such fuels are highly resistant to autoignition, they can be injected earlier than high cetane fuels to allow more time for fuel-air mixing. This is important for reducing soot emissions during high load operation. PPC with high octane fuels has been studied extensively [22–25], revealing that this combination can significantly reduce $NO_x$ and soot emissions while maintaining high thermal efficiency.

## 2.3 Reactivity Controlled Compression Ignition (RCCI)

The RCCI concept is a form of dual-fuel partially premixed combustion that has attracted considerable attention because it offers low $NO_x$ and soot emissions while maintaining high thermal efficiency [26, 27]. However, it also produces high HC and CO emissions, necessitating the use of an oxidation catalyst. The RCCI regime uses a blend of port-injected high-octane fuel with early direct-injected high-cetane fuel to handle autoignition and tune the combustion mixture's reactivity to better control combustion phasing. Two recently published review articles have summarized the progress to date in RCCI research, providing comprehensive overviews of this newly developed combustion mode [28, 29]. Much of the research into RCCI combustion has been performed using metal engines, including light- and heavy-duty engines, single-cylinder engines, and multi-cylinder engines. Multiple research groups have investigated the effects of low- and high-reactivity fuels on RCCI combustion [30–32], revealing that its combustion phasing is effectively controlled by mixture stratification, which can be influenced by varying the ratio of gasoline to Diesel, the Diesel injection timing, and the Diesel injection strategy. Despite its potential, there are concerns about the limitations of RCCI combustion when operating at low or high load due to low combustion efficiency, excessive rates of pressure rise, and mechanical engine constraints. Several studies have been conducted to find ways of alleviating these problems. Hanson et al. examined dual-fuel and single fuel RCCI combustion with an ignition improver at loads of 2 and 4.5 bar gross IMEP and various engine speeds [33]. At 4.5 bar gross IMEP, they were able to maintain a gross indicated thermal efficiency of 54% with low $NO_x$ and PM emissions; at 2 bar gross IMEP, the gross thermal efficiency was 44%. Splitter et al. [34] investigated the effects of single and double Diesel injection strategies on RCCI combustion using a bathtub-style piston at the low load of 4.75 bar IMEP, and found that double injection strategy reduced CO and HC emissions by 40%, while increasing thermal efficiency by 1% if the first injection in double injection strategy were between -30 [°ATDC] and -60 [°ATDC]. Using the same style of piston, the Splitter group [35] also showed that RCCI combustion could be maintained from low to full loads by reducing the compression ratio and top ring land height. Under these conditions, RCCI combustion achieved better thermal efficiencies and lower emissions of $NO_x$ and soot across the entire load map when compared to conventional Diesel combustion. Mokina et al. [36] also examined RCCI combustion from low to full load using a hydraulic VVA system to enable late inlet valve closing to reduce the effective compression ratio. Like Split-

ter et al., they found that RCCI improved thermal efficiency and reduced emissions of $NO_x$ and soot over the load sweep. While these results are promising, there is still a need to investigate the performance of RCCI concept under real-world operating conditions to verify its practicality. To this end, Hanson and Reitz [37] tested transient RCCI operation in a light-duty multi-cylinder engine. Their results showed that the engine could be operated in RCCI mode over a transient load step change without significant issues.

In addition to the metal engine studies discussed above, several optical engine studies have been performed to better understand fundamental details of RCCI combustion. Kokjohn et al. investigated RCCI combustion in an optical single-cylinder heavy-duty engine and used chemiluminescence and fuel-tracer planar laser-induced fluorescence (PLIF) imaging to characterize in-cylinder mixing and ignition processes [38]. They identified two initial ignition locations: inside the edge of the piston bowl rim and the squish region. Fuel distributions prior to ignition were measured by quantitative mixing measurement (PLIF), which showed a broad distribution of fuel reactivity . In a later work that incorporated kinetic analysis [39], the same group showed that fuel stratification was the dominant factor controlling the ignition process, followed by equivalence ratio stratification and temperature stratification. Tang et al. also highlighted the importance of fuel stratification in RCCI combustion based on simultaneous measurements of natural flame luminosity and emission spectra [40]. They found that the band spectra of OH, CH and $C_2/CH_2O$ became more distinct as fuel stratification increased. A recent work by Roberts et al. [41] identified the lean and rich limits of RCCI control authority using two different optical diagnostic methods: band-pass infrared imaging of emissions and chemiluminescence.

Finally, many studies have used detailed CFD modeling with reduced kinetic mechanisms to investigate RCCI combustion. CFD tools have provided insights into the locations of ignition sites, combustion processes, and the formation of intermediate species during combustion. Most of the published simulations of RCCI combustion were performed at the University of Wisconsin-Madison's ERC (Engine Research Center) using the KIVA-3V CFD code. Several publications [27, 30, 42, 43] have presented modeling results from this center that have helped to explain experimentally observed combustion behaviors. Other CFD studies have sought to optimize RCCI combustion. For example, Dempsey and Reitz [44] optimized RCCI combustion using gasoline and Diesel in a heavy-duty single-cylinder engine simulated by coupling the KIVA3V-CHEMKIN code to a multi-dimensional

algorithm (NSGA II). Their results indicated that clean and efficient RCCI combustion was achievable from 4 bar to 23 bar IMEP with a reduced compression ratio piston. Another computational work performed by Lim and Reitz [45] used the KIVA3V code coupled to NSGA II to simulate the same engine with a different compression ratio, and examined dual direct injection at 21 bar BMEP. The goal of this study was to optimize injection timings and mass splits to achieve low $NO_x$, soot, CO, and HC emissions while also minimizing the indicated specific fuel consumption (ISFC) and ringing intensity. The optimized conditions identified in this work were predicted to achieve a gross indicated thermal efficiency of 48.7% with very low $NO_x$, CO, and soot emissions as well as a reasonable maximum pressure rise rate (PRR) (12.6 bar/deg) and peak pressure (158 bar).

# Chapter 3

# Alcohol fuels in CI engines

Alcohol-based fuels have been used in combustion engines for more than a century. The three most commonly used fuel alcohols are methanol, ethanol, and butanol. They are of interest in automotive fields because they can be obtained from renewable sources, have low costs of production, and are environmentally friendly. Their high octane ratings make them less prone to engine knock and hence well suited as SI engine fuels, but mean that they are not naturally suited to CI operation. Various strategies for overcoming the difficulties of using pure alcohols in CI engines have been proposed, such as increasing compression ratios, adding ignition improvers, inlet air heating, and assisted ignition using a glow plug. Another common way of using alcohol fuels in CI engines is to adopt some kind of dual-fuel operating mode. Strategies of this kind are reviewed below.

## 3.1 Alcohol-Diesel blends

The most common way to use alcohol fuels in Diesel engines is to create uniformly premixed alcohol-Diesel blends that are injected into the cylinder through the fuel injector. The proportion of alcohols in such blends cannot exceed 30% because of their poor miscibility with Diesel [46–48]. These blends are also unstable, and may separate into distinct phases in the presence of water. To compensate for these problems, methanol-Diesel and ethanol-Diesel blends are often augmented with additives to improve their miscibility and eliminate the phase separation problem. The physical properties of alcohol-Diesel blends differ from those of pure Diesel: blends have lower viscosities, cetane numbers, and heating values. The use of blended fuels also has significant effects on combustion and emissions. Zhang et al. [49] investigated the effect of different alcohol-Diesel

blends on engine performance and emissions, and reported that the blends offered similar thermal efficiencies to pure Diesel but with much lower soot emissions. Sayin et al. [50] investigated engine performance and emissions for three different methanol-Diesel blends (M5, M10 and M15), and found that smoke opacity, hydrocarbon (HC) emissions, and carbon monoxide (CO) emissions were all reduced by using methanol-Diesel blends instead of Diesel. They also identified an optimum injection pressure that minimized break specific fuel consumption (BSFC).

## 3.2 Alcohol fumigation

In the alcohol fumigation approach, alcohol fuels are introduced into the intake air upstream of the manifold by spraying, carbureting, or injecting. This approach requires minor engine modifications involving adding low pressure fuel injectors, a separate fuel tank, and new fuel lines. There have been several experimental investigations into the effect of alcohol fumigation on engine performance and emissions. Most of these works used Diesel as an igniter, which was injected at the end of the compression stroke to ignite a premixed methanol/air mixture. Based on previous studies examining methanol-Diesel dual-fuel combustion, the parameter investigated most heavily in these works was the methanol substitution ratio [2, 51–54]. Common findings from these studies were that higher methanol substitution ratios reduced $NO_x$ and soot emissions but increased CO and HC emissions. Fumigation also tended to reduce brake thermal efficiency at low loads and increase it at high loads. Wei et al. [55] investigated the effects of single and double Diesel injection strategies on methanol-Diesel combustion. They concluded that a pilot injection in the double injection strategy could prevent misfire combustion while improving combustion stability and efficiency at low loads by increasing the cylinder pressure and temperature before the main combustion. Finally, several studies have shown that the use of alcohol fuels can significantly increase unburned alcohol emissions [55–57].

In addition to conventional alcohol fumigation combustion, there have been several studies on alcohol-Diesel RCCI combustion. Dempsey et al. [58] investigated RCCI combustion with gasoline-Diesel and methanol-Diesel mixtures in a single cylinder light-duty Diesel engine. They concluded that multiple injections should be used to achieve high thermal efficiencies and low $NO_x$ emissions when using methanol-Diesel RCCI. In addition, their results indicated that using an RCCI-optimized piston bowl increased both thermal efficiency and $NO_x$ emissions under all test conditions rela-

tive to the case with a stock piston during methanol-Diesel operation. The same group [59] also reported experimental studies on RCCI combustion with methanol-Diesel and methanol-methanol+cetane improver fuel systems. The combustion phasing of the methanol-methanol+cetane improver system was not significantly affected by the timing of the direct injection of the methanol+cetane improver mixture or the amount of mixture that was injected. Li et al. have presented multiple studies on methanol-Diesel RCCI combustion and the associated emissions using the KIVA-3V code. One of their early works in this area [60] examined the effects of the methanol mass fraction, SOI, and initial temperature in a methanol-Diesel RCCI engine. They concluded that the methanol mass fraction and SOI significantly affected the fuel's reactivity and the equivalence ratio distribution, and suggested that increasing the initial temperature could increase fuel efficiency while reducing emissions. In a separate work, the same group conducted a parametric study focusing on five parameters: the methanol fraction, SOI, initial temperature, initial pressure, and EGR level [61]. They identified the initial temperature and EGR level as the parameters with the strongest effect on fuel economy for methanol-Diesel RCCI combustion. However, the methanol fraction was the most practical and effective parameter to adjust in order to control combustion phasing CA50. A third study reported by this group focused on simultaneously varying two parameters, $R_P$ (the premixed fuel ratio) and the initial temperature, to explore their influence on methanol-Diesel RCCI combustion and the associated emissions [62]. It was found that methanol-Diesel RCCI has a narrow tolerable range of initial temperatures and thus requires very precise control over the intake conditions. In addition, they concluded that the trade-off between RI (ringing intensity) and EISFC (equivalent indicated specific fuel consumption) can be avoided by increasing $R_P$. Zou et al. [63] conducted a numerical study on the effects of three port-injected alcohol fuels (methanol, ethanol, and n-butanol) on RCCI combustion. They concluded that the combustion phasings of the methanol-Diesel and ethanol-Diesel were more sensitive to the premixed fuel ratio and less sensitive to the chosen single injection strategy than gasoline-Diesel and n-butanol-Diesel.

## 3.3 Alcohol direct injection

There has been relatively little research on direct injection of alcohol fuels in Diesel engines, and most studies that have been reported focused on systems in which the alcohol was injected at the end of the compression stroke. Ullman et al. [64] tested two direct methanol injection configurations (methanol with spark plug and methanol-Diesel) in two heavy-duty engines, and com-

pared the results to data for a reference Diesel engine during steady-state and transient operation. Replacing Diesel with methanol did not improve the equivalent brake specific fuel consumption (EBSFC) but significantly reduced PM emissions. However, in the absence of a catalyst system, the methanol-Diesel engines produced very high levels of unburned methanol and aldehydes, leading to high total HC and CO emissions. When catalyst systems were used, both methanol-Diesel and methanol with spark plug engines produced very low total HC and CO emissions. On March 2015, Stena Line launched Stena Germanica as the world's first methanol-Diesel dual-fuel operation ferry. The project has been carried out in collaboration with the engine manufacturer Wärtsilä, the ports of Gothenburg and Kiel as well as the world's largest producer and supplier of methanol, Methanex Corporation. The Wärtsilä's eight cylinder Diesel engine was converted to a methanol-Diesel engine with eight dual methanol/Diesel injectors mounted. MAN Diesel & Turbo developed a new MAN B&W ME-LGI dual-fuel engine on 2013. The engine involved high pressure direct injection two fuels with two separate injectors. One injector was used for the more sustainable high-octane fuels such as methanol, ethanol and Liquefied Petroleum Gas (LPG). The other injector was used to inject MGO (Marine Gas Oil), MDO (Marine Diesel Oil) or HFO (Heavy Fuel Oil) to ignite the high octane fuel. They reported that when operating on methanol, the ME-LGI significantly reduced emissions of $CO_2$, $NO_x$ and $SO_x$, and eliminated methanol slip. LoRusso and Cikanek [65] examined the direct injection of ethanol and methanol via a 4-hole injector in a single cylinder engine, with ignition by either a spark plug or a glow plug. Their results showed that the combustion of methanol or ethanol was initiated from the first spray plume ignited by the spark or glow plug. After that, the other three plumes released heat through flame propagation and then followed by compression ignition which is governed by chemical kinetics. At high loads, there was also a noticeable mixing-controlled combustion phase because the alcohol fuels were injected late in the compression stroke. The full load BMEP of the DI alcohol engine was 9 to 15 % greater than that for the baseline DI Diesel engine. In an effort to reduce HC and CO emissions while retaining the benefits of RCCI, early direct injection of both gasoline and Diesel with two separate injectors was investigated by Wissink et al. [66]. Direct injection of the two fuels yielded performance at least as good as port-injected gasoline RCCI, but with significantly lower $NO_x$ emissions and comparable emissions of HC and CO. CFD studies suggested that crevices were the main source of the observed HC emissions. Consequently, good spray targeting could potentially reduce the HC emissions of such systems. No studies on early direct injection of alcohol fuels have yet been reported, but this approach warrants

investigation because of its potential to reduce HC and CO emissions while maintaining the established benefits of RCCI combustion.

# Chapter 4

# Gaseous fuels in CI Engines

Multiple gaseous fuels are suitable for the engine operation such as biogas, NG, synthesis gas (syngas) and hydrogen ($H_2$). NG/biogas in particular has been studied extensively and has been used in both spark-ignition (SI) and compression-ignition (CI) engines. Broadly speaking, there are two classes of SI engines that can use NG/biogas: conventional engines that have undergone bi-fuel conversion for light duty applications, and dedicated gas SI engines for heavy duty applications. In bi-fuel engines, the gasoline fuel system is often retained and a gas injection system is built into the intake manifold. In such cases, the original engine management system is usually used to control gas flow, and a gas mixer is added to ensure thorough gas/air mixing. The gasoline fuel injector is disabled when the engine is running on gas. In contrast, dedicated gas SI engines are optimized to operate with gas alone. The gas is normally either port-injected or injected into the intake manifold and then ignited by a spark plug. Volvo FE NG was equipped with a new Euro 6 engine using compressed natural gas together with spark plug. Scania also released a dedicated gas-powered engine and the combustion of gaseous fuel was initiated using spark plug. CI engines that use NG/biogas typically operate in a dual-fuel mode. Dual-fuel engines use two different fuels, both of which may be directly injected. Alternatively, the high-cetane fuel can be directly injected while the high-octane fuel is port-injected. Since dual-fuel gas engines are the main focus of this thesis work, the literature review below deals primarily with the dual-fuel field.

## 4.1 Gas fumigation

### 4.1.1 Conventional gas-Diesel engines

Traditionally, in gas-Diesel dual-fuel engines, the compressed natural gas/biogas is injected into the intake manifold during the intake stroke, then the gas and air mixture is compressed during the compression stroke. A pilot Diesel injection performed at the end of the compression stroke acts as an ignition source. This type of dual-fuel engines is not a recent concept and several review papers have been written [67–70]. A typical rate of heat release (RoHR) trace for this type of dual-fuel combustion is depicted in Figure 4.1. The combustion process can be divided into five main phases: pilot Diesel fuel combustion, NG combustion surrounding the pilot spray, flame propagation through the premixed NG/air mixture, autoignition of end gas, and late mixing-controlled combustion. Karim [71] was the first to describe a well-known dual-fuel combustion process in terms of the first three phases mentioned above; eng gas autoignition was recognized as a distinct phase somewhat later [72]. Because the progression of the end gas autoignition phase is governed by the rates of chemical reactions, it occurs more rapidly than flame propagation. It is followed by a much slower combustion phase that may reflect the combined effects of late mixing-controlled combustion and slow combustion of NG from crevices in the expansion stroke.

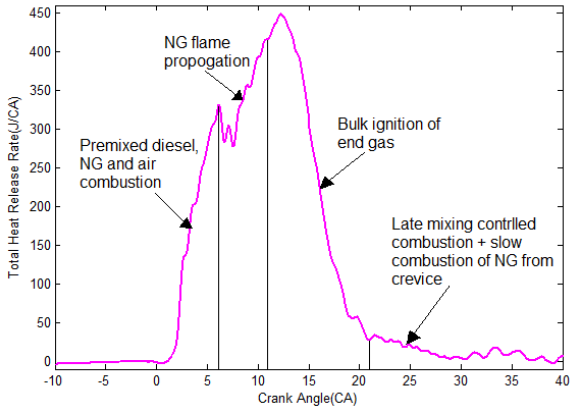


Figure 4.1: A typical rate of heat release plot for conventional gas-Diesel combustion

Studies on gas-Diesel dual-fuel engines have examined several parameters to determine their effects on engine performance and emissions, including the pilot injection quantity, pilot injection timing, intake charge temperature, EGR level, air excess factor, compression ratio, NG supplement ratio,

engine load, and speed [69, 70, 73–84]. A common issue with NG/biogas engines is the poorer performance and higher unburned hydrocarbon and carbon monoxide (CO) emissions at low loads due to much leaner mixtures than that at high loads. This problem can be alleviated by increasing the pilot injection quantity, preheating the intake charge, and using hot EGR, etc [73,76,79]. At high loads, significant improvements in dual-fuel combustion have produced corresponding improvements in both engine performance and emissions of unburned HC and CO emissions [84, 85]. Contrasting results have been reported regarding the thermal efficiency (at high loads) of dual-fuel combustion. Some studies have concluded that the thermal efficiencies of dual-fuel operation are similar to those for pure Diesel combustion [84, 86], whereas others claim higher thermal efficiencies than for pure Diesel [68,85]. This discrepancy may be due to the use of different engine setups, natural gas induction systems, and different equivalence ratios by different research groups. One issue with dual-fuel engines operating at very high loads is the tendency for knocking, possibly due to end-gas autoignition [87]. Parameters such as the charge temperature, pilot injection quantity and injection timing may all have important effects on the onset of knock [88]. Compared to pure Diesel cases, low levels of $NO_x$ emissions for gas-Diesel dual-fuel combustion have been reported by different authors [78, 83, 84, 89]. At low loads, much lower $NO_x$ emissions (around 50% reduction) have been observed for gas-Diesel dual-fuel cases than for pure Diesel cases [70]. Particulate matter (PM) is maintained at a low level for gas-Diesel dual-fuel engines due to the presence of premixed NG/biogas and air, together with only a small amount of Diesel injected. However, it should be noted that the main unburned HC emission from NG/biogas engines is methane, which is largely inert in terms of photochemical smog formation but is roughly 28 times more potent than carbon dioxide as a GHG.

### 4.1.2 Gas-Diesel RCCI engines

In gas-Diesel RCCI combustion, port-injection of gaseous fuel is combined with early direct injection of Diesel to control autoignition and the charge mixture's reactivity. A good combustion process can be achieved by changing the ratio of NG and Diesel to vary the fuel mixture's reactivity. Figure 4.2 shows a representative NG-Diesel RCCI RoHR trace with distinct low temperature heat release (LTHR) and high temperature heat release (HTHR) regions. Ignition processes that produce RoHR traces of this type were described as two-stage ignition processes by Glassman and Yetter [90],

and have been observed for various hydrocarbons (but not for methane and ethane). The first and second ignitions are associated with chemical reactions and the thermal conditions, respectively. The LTHR is a small heat release (also known as a cool-flame heat release), which is characteristic of low temperature Diesel combustion. The HTHR is known as the main heat release, and can be divided into a premixed combustion phase and a phase associated with slow combustion of NG from crevices in the expansion stroke.

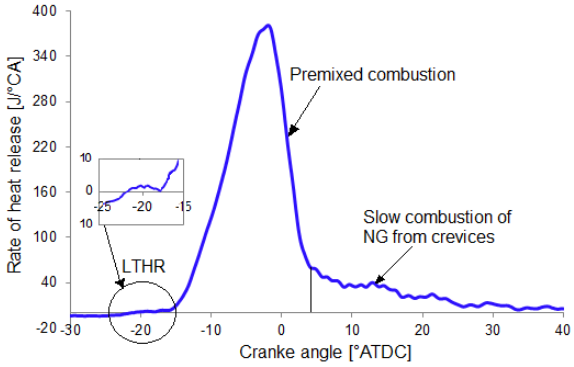


Figure 4.2: A typical NG-Diesel RCCI rate of heat release curve

Several studies have explored the effects of different engine parameters on engine performance and emissions when using NG-Diesel RCCI combustion. Nieman et al. [91] compared the effects of single and double Diesel injection strategies, and found that a double injection strategy with a very late second Diesel injection was necessary to achieve reasonable performance at high load (23 bar IMEP) while maintaining an acceptable maximum pressure rise rate (PRR) and peak pressure. However, soot emissions were high under these conditions. The single injection strategy produced dramatically lower soot emissions but had a lower maximum load (21 bar IMEP) while maintaining an acceptable maximum PRR and peak pressure. NG-Diesel RCCI combustion was studied up to rated power conditions by Zoldak et al. using CFD [92]. They showed that NG-Diesel RCCI combustion achieved better fuel economy and lower $NO_x$ and soot emissions than the baseline Diesel case, with an acceptable maximum PRR and peak pressure. Ryan Walker et al. [93] reported an experimental comparison of methane-Diesel and gasoline-Diesel RCCI combustion with combustion phasings (CA50 values) of 0 and 4 °ATDC in the absence of EGR. They found that the maximum load for methane-Diesel RCCI combustion (13.7 bar IMEP) while remaining below the engine's maximum PRR limit was substantially higher than that for gasoline-Diesel RCCI combustion (6.9 bar

IMEP). Additionally, COV of IMEP and maximum PRR measurements indicated that methane-Diesel RCCI combustion was significantly more stable than gasoline-Diesel RCCI combustion. Doosje et al. [94] performed experiments with NG-Diesel RCCI combustion at different engine speeds and loads, and identified a "sweet point "for HC and CO emissions during the SOI sweep. However, this "sweet point "also produced the highest measured $NO_x$ emissions. To maintain $NO_x$ emissions below the Euro VI upper limit (0.46g/kWh), the SOI needed to be advanced from the HC "sweet point "SOI. Additionally, the gas quality seemed to have only a small effect on gas-Diesel RCCI combustion. Dahodwala et al. [95] studied NG-Diesel RCCI combustion at loads of 6 and 14 bar BMEP. The results obtained at 6 bar BMEP indicated that the combustion phasing (CA50) could be easily controlled by varying the levels of NG substitution and EGR. In the high load case (i.e., at 14 bar BMEP), the maximum PRR was the limiting factor for RCCI combustion. Li et al. [96, 97] published two papers on the application of dynamic $\phi - T$ in NG-Diesel RCCI combustion using KIVA4. The first paper examined the effects of five parameters – the NG fraction, first SOI timing, second SOI timing, second injection duration, and EGR level – and identified the EGR level and NG fraction as the most influential [96]. The second paper [97] examined four parameters – the NG fraction, first SOI, Diesel split fraction, and EGR level – with the aim of minimizing NO and soot emissions from a NG-Diesel RCCI engine. The NG fraction and EGR level were identified as the most important parameters in this case.

## 4.2 Gas direct injection

Three different combustion chamber layouts can be used for gas-Diesel dual-fuel direct injection: a central gas injector with a side-mounted pilot injector, a central pilot injector with a side-mounted gas injector, or a unitary central injector for both Diesel and NG. Figure 4.3 shows a combustion chamber layout of the first kind. Due to the poor self-ignition capacity of the gaseous fuel, a small amount of Diesel is injected via the side-mounted pilot injector and used to ignite the injected gas. In this type of engine, high pressure gas is injected after charged air has been compressed as in normal Diesel engines. Therefore, the gas fuel burns mostly in the diffusion combustion mode, as in a normal Diesel engine [98–100].

The design shown in Figure 4.3 can't use pure Diesel fuel at high loads because the side-mounted Diesel injector cannot produce fuel jets capable of utilizing the air in the cylinder in a short time. The so-called "H-Process"combustion process (Figure 4.4) was invented by Hsu to address

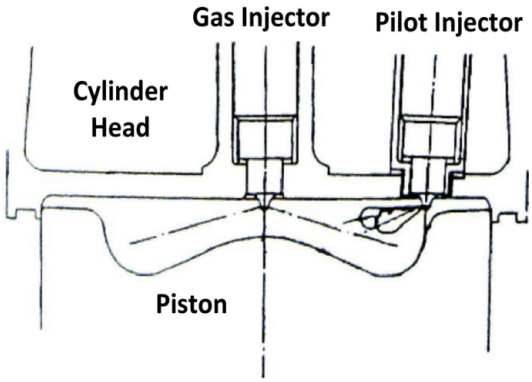


Figure 4.3: High-pressure center-mounted gas injector engine combustion chamber layout [98]

this issue. When operating on pure Diesel fuel, combustion proceeds as in a conventional Diesel engine. However, when operating in dual-fuel mode, the gas fuel is injected into the combustion chamber at an angle to the cylinder diameter to produce a swirling motion in the cylinder charge, which facilitates mixing in the cylinder. In contrast to the diffusion combustion produced by a center-mounted gas injector mounted as described above, the side-mounted gas injector injects the gas fuel before the pilot injection to enable premixing with air, leading to lean-burn premixed combustion [101].

While both concepts described above use two injectors, it is also possible to use a unitary injector in a high pressure direct injection gas-Diesel engine. Westport Innovations Inc. has developed a system for the high-pressure direct-injection (HPDI) of NG. The HPDI system consists of two concentric injectors, with Diesel introduced in the inner injection system and natural gas in the outer injection system. A schematic of the injector nozzle is shown in Figure 4.5. In most studies with HPDI injectors, the injection of NG occurred late in the compression stroke, so most of the NG was burned in diffusion mode [102–104].

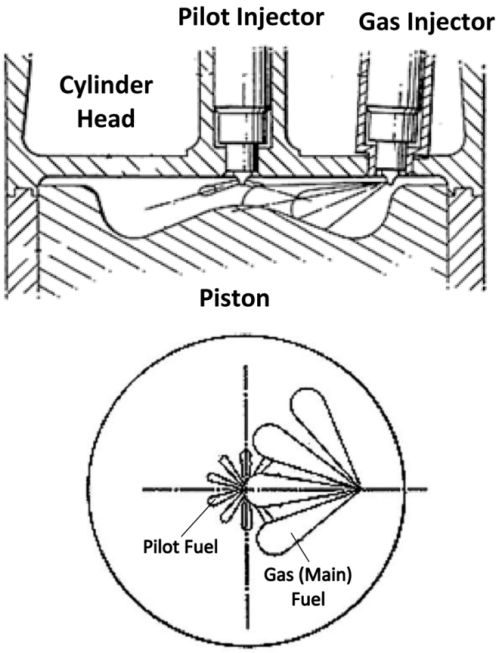


Figure 4.4: The "H-Process"side-mounted gas injector engine combustion chamber layout [105]

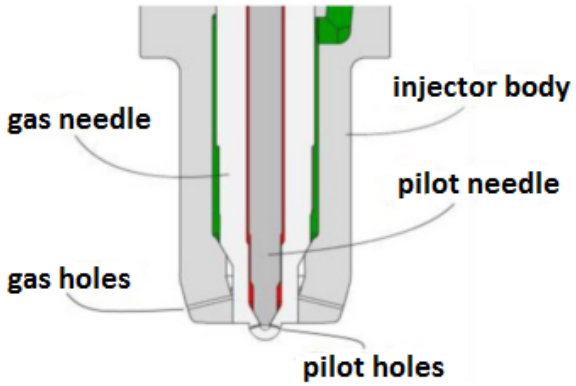


Figure 4.5: Schematic of the HPDI injector nozzle [102]

# Chapter 5

# Experimental Setup

This chapter provides an overview of the experimental apparatus and testing methods used in this work.

## 5.1 Engine setup

All experiments presented in this thesis were conducted in the same heavy-duty single cylinder cell but with two different engine displacement volumes. Studies using gaseous fuels (papers I - IV) were performed with an engine displacement of 2.02L to mimic the Volvo Powertrain D12C engine. The final study with methanol was done with a displacement volume of 2.13L to mimic the Volvo Powertrain D13 engine. Engine specifications for the two setups are given in Table 5.1.

Table 5.1: Engine specifications

| Engine type | Single cylinder | Single cylinder |
|---|---|---|
| Bore [mm] | 131 | 131 |
| Stroke [mm] | 150 | 158 |
| Connecting rod [mm] | 260 | 267.5 |
| Compression ratio | 17:1 and 14:1 | 16.6 |
| Number of valves | 4 | 4 |

Two schematic layouts of the engine are shown in Figures 5.1 and 5.2. The first layout was used for gaseous fuel studies and the second for methanol study. Both setups were controlled using an AVL PUMA OPEN system. The intake air was passed through a screw compressor to establish the required boost pressure, followed by a dryer to remove water, an air conditioning unit to heat the air to the required temperature, and finally a

plenum to eliminate pressure oscillations. The recirculated exhaust gas was cooled by the engine's cooling water before entering the intake system. The temperature of the exhaust gas after cooling depended on the amount of EGR used and the engine load. The mass flow of NG/$CH_4$ in Figure 5.1 was measured using a Micro Motion CMD025 Coriolis flow meter, while the Diesel mass flow was calculated based on mass and time measurements acquired using an AVL 733S dynamic fuel balance. In the second engine setup, the mass flows of methanol and pilot Diesel were measured using two separate AVL 733S dynamic fuel balances.

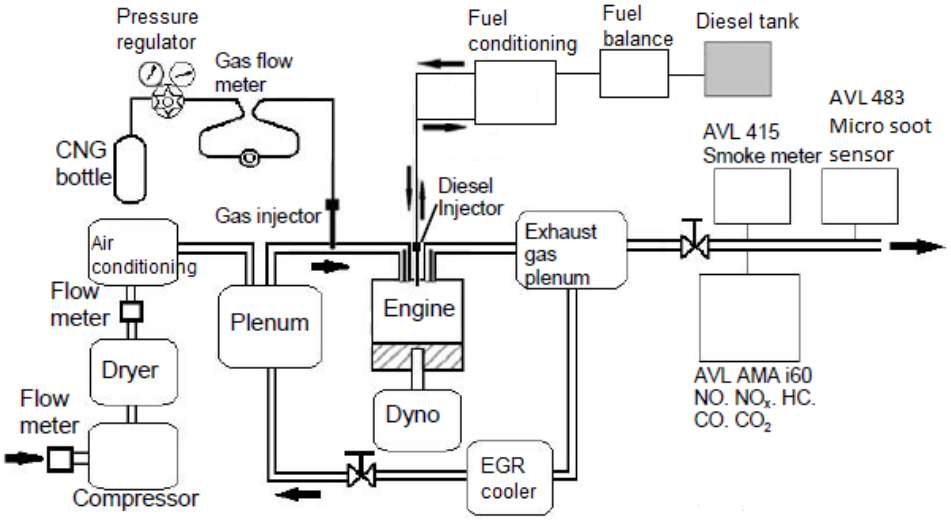


Figure 5.1: Schematic layout of the engine as used in papers I - IV

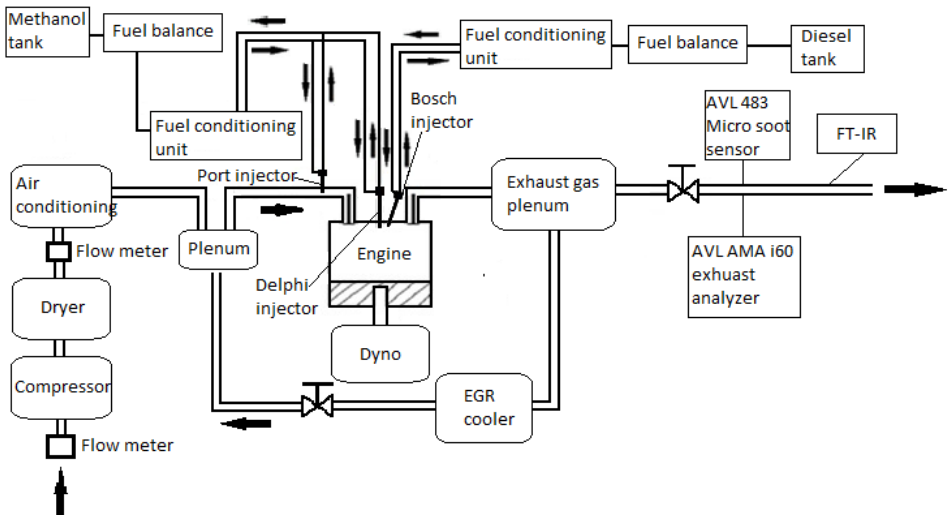


Figure 5.2: Schematic layout of the engine as used in paper V

## 5.2 Fuel and injection system

Four fuels were used during this work. Most of the experiments were performed with NG as the high-octane fuel (papers I - IV). In paper I, pure $CH_4$ was also tested as the high-octane fuel to mimic biogas. In paper V, methanol was used as the high-octane fuel. All experiments used Swedish environmental class 1 Diesel (MK1) fuel as the high-cetane fuel. Some key properties of these fuels are listed in Table 5.2. The properties of the NG were calculated based on its composition: its density was obtained from the ideal gas law, MON was calculated using previously published equations [106], and its heating value could be calculated from its composition since each compound's heating value was known.

Table 5.2: Characteristics of the $CH_4$, NG, methanol and Diesel fuels used in the experiments

| Fuel | $CH_4$ | NG | Methanol | Diesel (MK1) |
|---|---|---|---|---|
| Viscosity [$mm^2/s$] (at 40°C) | - | - | 0.58 | 1.4-4 |
| Density [$kg/m^3$] | 133.9 @20MPa | 155.7-196.6 @20MPa | 0.792 | 800-830 |
| RON [-] | 120 | - | 106 | - |
| MON [-] | 120 | 122.5-122.6 | 92 | - |
| Cetane number [-] | - | - | 3.8 | $\geq$51 |
| Lower heating value [MJ/kg] | 50 | 46.68-46.93 | 20.0 | 43.1 |
| Enthalpy of vaporization [KJ/kg] | $\sim$509 | - | $\sim$1100 | $\sim$270 |

### 5.2.1 NG/$CH_4$ and Diesel

Two gas injectors were mounted on the intake manifold and controlled by a Bosch control unit. A pressure regulator was used to reduce the gas pressure from 200 bar to 14 bar for proper operation of the gas injector. The NG composition is given in Table 5.3. The second and third columns detail the composition of the NG used in papers I - III and IV, respectively. The Diesel fuel used in papers I - IV was delivered using a common rail DI system capable of delivering up to five injections per cycle with an injection pressure of up to 2700 bar. The specifications of the Diesel injector are given in Table 5.4.

Table 5.3: Composition of the NG

| Compound | Percent in NG (v/v) | |
|---|---|---|
| Methane | 88.8% | 87.9% |
| Ethane | 5.6% | 5.9% |
| Propane | 2.4% | 2.6% |
| Isobutane | 0.3% | 0.36% |
| Butane | 0.5% | 0.59% |
| Pentanes | 0.15% | 0.21% |
| Carbon dioxide | 1.2% | 1.5% |
| Carbon monoxide | 0.4% | 0.07% |
| Oxygen | 0.15% | 0.07% |
| Nitrogen | 0.5% | 0.8% |

Table 5.4: Diesel injector specifications

| | |
|---|---|
| Number of holes | 5/7 |
| Steady flow rate at 100 bar [L/min] | 2 @ 5; 2.15 @ 7 |
| Hole diameter [mm] | 0.256 @ 5; 0.225 @ 7 |
| Injection pressure [Bar] | 1000 |
| Spray angle | 145° |

### 5.2.2 Methanol and Diesel

The final study involved both port-injected and direct-injected methanol. Four port injectors were needed to deliver the required amount of fuel. The port injectors' specifications are shown in Table 5.5. To facilitate comparison with the methanol-Diesel results, pure Diesel experiments were performed using a conventional Delphi Diesel injector. The pilot Diesel injection was always delivered with a Bosch injector. The engine was thus fitted with two common rail DI systems, one for methanol and one for pilot Diesel injections; both were controlled by Vision. The specifications of the Delphi injectors are shown in Table 5.6.

Table 5.5: Methanol port injector specifications

| | |
|---|---|
| Number of holes | 6 |
| Static flow rate at 3 bar (cc/min) | 548 |
| Injection pressure [bar] | 7.8 |
| Spray angle | 25° |

Table 5.6: Common rail injector specifications

| Common rail injector | 1(Diesel) | 2(Methanol) | 3(Methanol) |
|---|---|---|---|
| Number of holes | 6 | 7 | 2 |
| Flow number @ 100 bar | 2.3 | 3.0 | 0.6 |
| Injection pressure [bar] | 1500-2000 | 800-1200 | 800-1400 |
| Spray angle | 150° | 145° | 51.4° |

## 5.3 Emissions analyzer

The exhaust concentrations of $NO_x$, CO, $O_2$, $CO_2$, and HC, and the intake $CO_2$ concentration, were measured using an AVL AMA i60 emissions analyzer. The amount of EGR applied was calculated based on the measured intake and exhaust $CO_2$. Soot emissions were measured using an AVL 415 smoke meter in papers I - III, where very low soot emissions were observed in most of the test cases. Therefore, in papers IV - V, soot levels were measured with an AVL 483 Micro Soot Sensor. This instrument can detect soot particles at concentrations of 5$\mu$g-50 mg /m$^3$. The detector details for each compound are shown in Table 5.7. A heated sample (190°C) was fed to the i60 FID and CLD detectors, whereas a cooldown sample was employed for the rest of detectors in the AMA i60 analyzer. Levels of unburned methanol in Paper V was measured using FT-IR.

Table 5.7: Exhaust gas measurement devices

| | |
|---|---|
| $NO_x$ | CLD i60 HHD SLQ |
| CO | IRD i60 CO H |
| $CO_2$ | IRD i60 $CO_2$ H |
| $O_2$ | PMD i60 $O_2$ |
| HC | CUTTER FID i60 HHD |
| $CH_3OH$ | FT-IR |
| Soot | AVL 415 smoke meter<br>AVL 483 Micro Soot Sensor |

## 5.4 Data acquisition

Several engine parameters were measured during the experiments. A Kistler 7061B piezo-electric pressure sensor was mounted in the cylinder head to monitor the cylinder pressure in order to enable heat release rate analyses and in-cylinder temperature calculations for papers I - IV. The in-cylinder pressure measurements in the final measurement campaign (paper V) were performed with an AVL QC34C pressure sensor. The intake pressure was measured using a Kistler 4045A5 piezo-resistive pressure sensor. Both high temporal resolution sensor readings were collected using a D2T Osiris data acquisition system with a sampling interval of 0.1 CAD. The cylinder pressure traces were averaged over 100 cycles to smooth the pressure data. In papers I - III, the Osiris software was used to perform all calculations relating to the pressure traces. Since heat losses were not considered in the rate of heat release calculations, the calculated rate of heat release (RoHR) was the apparent one. In papers IV and V, the gross heat release rate was calculated using a Matlab script based on the equations in Heywood [107]. This script accounts for heat losses to the cylinder walls using the Woschni heat transfer model. The gross RoHR calculation is described in the Appendix A.

Some engine parameters were only recorded with low temporal resolutions. For instance, all temperatures (water inlet/outlet, intake air, oil, exhaust and EGR) were measured by resistance thermometer PT100.

## 5.5 Operating conditions

Before running the engine, it was heated until the coolant water and engine oil temperatures reached 80°C. The engine was then started and combustion was allowed to proceed until the coolant water and engine oil reached 85 and 90 °C, respectively. After that, the real measurements began.

### 5.5.1 Conventional gas-Diesel operation

At the beginning of this project, conventional gas-Diesel combustion was examined to check the performance and emissions of the Volvo D12C single cylinder engine. Papers I and II of this thesis describe these studies. The main test conditions used in this work are shown in Table 5.8.

Table 5.8: Test conditions for conventional gas-Diesel operation

| | |
|---|---|
| Engine speed [rpm] | 1500 |
| BMEP [bar] | 6 and 12 |
| Diesel injection pressure [bar] | 2000 |
| Diesel SOI (electrical signal) [BTDC] | 6 |
| Compression ratio | 17:1 |
| Absolute Intake pressure [bar] | 1.0 @ 6 bar BMEP<br>1.5 @ 12 bar BMEP |

### 5.5.2 NG-Diesel RCCI operation

The second part of this thesis deals with RCCI combustion. Two studies were performed to investigate NG-Diesel RCCI combustion. The first sought to establish a general understanding of the in-cylinder mixture properties required to realize NG-Diesel RCCI combustion by varying different engine parameters. The second study was a continuation of the first, and was intended to better control the combustion phasing and extend the operational range of the NG-Diesel RCCI system by using late inlet valve closing. These two studies are presented in papers III and IV of the thesis, respectively. Engine parameters such as engine speed, load, intake pressure, and compression ratio were varied during the first RCCI combustion study. Table 5.9 lists the test conditions used in that work. A double Diesel injection strategy was used, and Diesel was injected quite early in the compression stroke. In the second study, the experimental tests were conducted at different IVC timings (-154, -141, -133, -124, and -111 °ATDC) and engine speeds (1200, 1500, and 1800 rpm). In addition, different characteristic investigations (e.g. Diesel injection strategy, IVC at various equivalence ratios, engine speeds, and combustion phasings) were performed at 1200 rpm and 9 bar BMEP. Finally, the scope for operational load extension was tested using an engine speed of 1500 rpm with IVC at -124 °ATDC. The test conditions used in this work are shown in Table 5.10. Figure 5.3 presents a graphical depiction of the double Diesel injection profile that was used in papers III,IV, and V. The first and second injections were designated pilot injection 1 (PI1) and pilot injection 2 (PI2), respectively. The SOI of PI1 was much advanced than that of PI2.

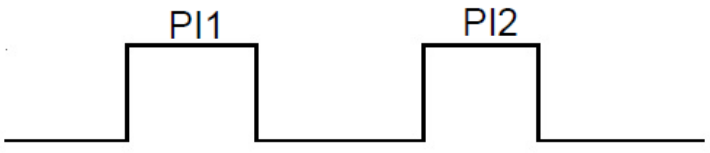


Figure 5.3: The double Diesel injection profile

Table 5.9: Test conditions for NG-Diesel RCCI operation in Paper III

| Engine speed [rpm] | Load BMEP [bar] | Diesel injection pressure [bar] | EGR [%] | Intake pressure [bar] | Compression ratio |
|---|---|---|---|---|---|
| 1200 | 7−10 | 1000 | 42 | 1.7−1.9 | 17:1 & 14:1 |
| 1500 | 7−10 | 1000 | 42 | 1.7−1.9 | 17:1 & 14:1 |
| 1800 | 7−10 | 1000 | 42 | 1.7−1.9 | 17:1 & 14:1 |

Table 5.10: Test conditions for NG-Diesel RCCI operation in paper IV

| | |
|---|---|
| Engine speed [rpm] | 1200, 1500, 1800 |
| BMEP [bar] | 9 and 14 |
| Diesel injection pressure [bar] | 1000 |
| Diesel injection strategy | single/double |
| Compression ratio | 17:1 |
| EGR [%] | 23-32 |
| IVC [°ATDC] | -154, -141, -133, -124, -111 |

### 5.5.3 Methanol-Diesel RCCI operation

The final study (Paper V) included in the thesis investigated the performance and emissions of methanol-Diesel RCCI combustion using three different methanol injection configurations in the Volvo D13 single cylinder engine. The tested methanol injection configurations were port injection into the intake manifold, direct injection during the intake stroke (referred to as DI_E), and direct injection during the compression stroke (referred to as DI_L). A double Diesel injection strategy was used in all the methanol-Diesel experiments. Conceptual illustrations of the three different methanol-Diesel injection strategies are shown in Figure 5.4. All the methanol-Diesel experiments were performed at a constant engine speed of 1500 rpm. Experiments on the effects of variables such as the methanol injection pressure, Diesel start of injection (SOI), methanol substitution percentage (MSP), and Diesel duration split ratio were performed at 5 bar IMEP and an in-

take temperature of 60 °C. In addition, a load sweep was performed for the methanol port injection and DI_L configurations, and the results obtained were compared to data for a reference Diesel case. The operating conditions used in this study are shown in Table 5.11.

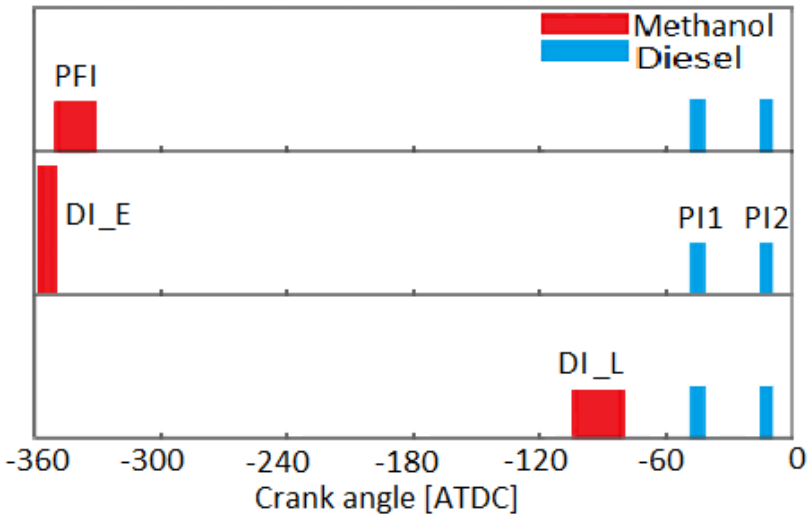


Figure 5.4: Conceptual illustration of the injection strategies used in paper V

Table 5.11: Test conditions for methanol-Diesel RCCI operation

| | |
|---|---|
| Engine speed [rpm] | 1500 |
| Compression ratio | 16.6 |
| IMEP [bar] | 5, 8, 10 and 14 |
| Diesel injection pressure [bar] | 500 |
| Methanol injection pressure [bar] | 7.8 @ port injection<br>800 @ DI_E<br>800-1200 @ DI_L |
| Diesel injection strategy | double |

# Chapter 6

# 3D Dual-Fuel Combustion Models

This chapter reviews 3D CFD models for dual-fuel combustion. It is divided into two parts: one discussing a model for conventional gas-Diesel combustion developed at Chalmers, and one discussing the commercial ANSYS FORTE 18.1 software package for NG-Diesel RCCI combustion.

## 6.1 Overview of 3D CFD models

### 6.1.1 The conventional gas-Diesel 3D model

The 3D dual-fuel combustion model was developed at Chalmers to simulate CI engines and predict their performance and emissions during dual-fuel combustion. The model is based on the KIVA code coupled with CHEMKIN II. The sub-models implemented in the KIVA code are shown in Table 6.1. The only model presented here is the dual-fuel combustion model because the other sub-models have already been used with the KIVA-3V and KIVA-4V codes for other applications and are described elsewhere [108–110].

The dual-fuel combustion model is based on two coupled modes: the "conventional"partially premixed reactor spray combustion mode, PaSR, [108] and the flame propagation mode [111]. To illustrate the model's development, it is helpful to start by considering a mass balance equation without a spray source:

$$\frac{\partial c_m}{\partial t} + \nabla\cdot(c_m \boldsymbol{u}) = \nabla\cdot[\rho D \nabla(\frac{c_m}{\rho})] + \dot{\rho}_m^{c1} + \dot{\rho}_m^{c2} \tag{6.1}$$

$$c_m = \rho_m / W_m, m = 1, \ldots, N_m$$

Here, $\rho$ is the density of the gas mixture, $\dot{\rho}_m^{c1} + \dot{\rho}_m^{c2}$ represent the chemical sources corresponding to the two combustion modes mentioned above, $c_m$ is the mole density of species m, $W_m$ is its molecular mass, $\boldsymbol{u}$ is the velocity vector, and $N_m$ is the number of species in the mixture.

Table 6.1: Computational sub-models used in the conventional dual-fuel combustion model

| | |
|---|---|
| Turbulence model | $\kappa$ - $\epsilon$ model |
| Breakup model | Hybrid KH-RT model |
| Droplet collision model | Droplet trajectories interaction |
| Spray/wall interaction model | Standard KIVA model |
| Wall heat transfer model | Standard KIVA model |
| Evaporation model | Single component, KIVA model |
| Spray combustion | PaSR coupled with chemical kinetics |
| Flame propagation | TFC/Premix flame model for aspirated fuel |
| Fuel composition | Methane, natural gas/DOS (Diesel oil surrogate) |

From the dimensionality condition for the chemical terms in Eq.(6.1), it follows that

$$\dot{\rho}_m^{c1} \approx \frac{c_m}{\tau_{c1}}, \dot{\rho}_m^{c2} = \frac{c_m}{\tau_{c2}}, \dot{\rho}_m^{c1} + \dot{\rho}_m^{c2} = \frac{c_m}{\tau_c} \tag{6.2}$$

where the characteristic times of the different combustion modes $\tau_{c1}, \tau_{c2}$ and the overall process $\tau_c$ are related by

$$\tau_c = \frac{\tau_{c1}\tau_{c2}}{\tau_{c1} + \tau_{c2}} = \frac{1}{2}H(\tau_{c1}, \tau_{c2}) \tag{6.3}$$

where $H(\tau_{c1}, \tau_{c2})$ is a harmonic mean.

If $\tau_{c1} \gg \tau_{c2}$, Eq.(6.3) reduces to $\tau_c \cong \tau_{c2}$, implying that mode 2 is the dominant combustion process. For the general case, Eq.(6.3) "interpolates" between the two mode rates. This approach is more accurate than "switching" between the model combustion rates, as described in [112], $\dot{\rho}_m^c = max(\dot{\rho}_m^{c1}, \dot{\rho}_m^{c2})$.

### 6.1.2 NG-Diesel RCCI 3D model

ANSYS FORTE is an advanced CFD simulation package for realistic simulation of CI engine performance and emissions, which incorporates ANSYS Chemkin-Pro solver technology. It enables multi-component fuel models to be combined with comprehensive spray dynamics - without sacrificing simulation time-to-solution. The sub-models implemented in ANSYS FORTE have been well validated against experimental data over a broad range of conditions.

## 6.2 Chemical kinetic mechanisms

### 6.2.1 The conventional gas-Diesel mechanism

CHEMKIN II code [113] was used to construct and validate dual-fuel (NG-Diesel and methane-Diesel) chemical kinetic mechanisms involving 80 species and 384 finite-rate reactions. Because Diesel oil consists of numerous aliphatic and aromatic compounds, it is necessary to use surrogate fuel models in numerical simulations. The physical properties of the liquid Diesel oil surrogate (DOS) used in the simulations were considered to be the same as the Diesel oil DI model from the KIVA code fuel library. The DOS vapor thus consisted of 70% *n*-heptane ($C_7H_{16}$) and 30% toluene ($C_7H_8$). The aliphatic components of real Diesel were represented by *n*-heptane, which has a similar cetane number ($\sim$56) to conventional Diesel. Toluene was used to represent the aromatic components, which contributed significantly to soot formation. NG was assumed to be a four-component mixture of methane, ethane, propane, and *n*-butane with the composition listed in Table 5.3. The chemical kinetic mechanisms were validated by comparing predicted laminar flame speeds and ignition delay times to experimental measurements acquired at atmospheric pressure and in a shock tube, respectively. Paper II includes details of the validation of the kinetic mechanisms.

### 6.2.2 The NG-Diesel RCCI mechanism

Chemkin-Pro and Reaction Workbench were used to generate a reduced mechanism from the Model Fuel Library (MFL). The MFL mechanism was a Diesel master mechanism named "Diesel_PAH_$NO_x$", which contained 5155 species. The Batch rector model in Chemkin-Pro was used to reduce the mechanism, assuming the following ranges of conditions: pressure 20-100 bar; temperature 600-1800 K; equivalence ratio 0.5-2, and EGR 0-30%. The final reduced mechanism contained 400 species and 3097 reactions. The surrogate Diesel was consisted of n-heptane as the chemical representation

and n-tetradecane as the physical property representation for Diesel spray and vaporization. NG was represented by $CH_4$.

## 6.3 Engine simulation mesh

For the conventional gas-Diesel cases, engine simulations were performed on a 51.4° sector mesh for both NG-Diesel and methane-Diesel mixtures to capture one spray/flame region of the 7-orifice nozzle. This mesh had 74812 cells at bottom dead center. Since a five-hole injector was assumed in the NG-Diesel RCCI simulation, the numerical work was performed on a 72° sector mesh with 259090 cells at bottom dead center. Both sector meshes are shown in Figure 6.1: the 51.4° sector mesh on the left, and the 72° sector mesh on the right.

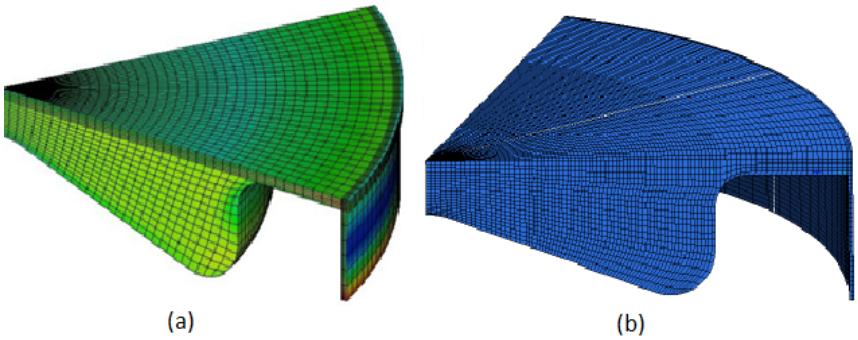


Figure 6.1: 51.4° and 72° sector computational meshes

# Chapter 7

# Results

This chapter provides an overview of the results obtained during the project.

## 7.1 Conventional gas-Diesel combustion

As a starting point, the combustion and emissions of conventional NG-Diesel and $CH_4$-Diesel dual-fuel systems were investigated using a Volvo D12C single cylinder engine. A pilot Diesel injection near top dead center was used to achieve ignition. Paper I presents some of the results from this study. The main parameter investigated was the NG/$CH_4$ mass ratio in the gas-Diesel mixtures. The experiments were performed at a constant engine speed of 1500 rpm and two different load points: 6 bar and 12 bar BMEP. Figure 7.1 shows the in-cylinder pressure and apparent rate of heat release (RoHR) traces obtained at 6 bar BMEP. The only parameter varied here was the NG mass ratio in the fuel mixture. At this light load, there was sufficient time for premixing during the ignition delay period in the pure Diesel case, so the pure Diesel combustion was predominantly premixed, with a minor contribution from diffusion combustion. Consequently, the NG-Diesel case with an NG mass ratio of 63.3% offered little advantage over the pure Diesel case. Increasing the NG mass ratio to 85.7% deteriorated combustion, yielding slow combustion and a long combustion duration.

At the intermediate load of 12 bar BMEP, both NG and $CH_4$ were tested as high-octane fuels. Figures 7.2 and 7.3 show the pressure and apparent RoHR traces for the NG-Diesel and $CH_4$-Diesel, respectively. The RoHR traces shown in Figure 7.2 indicate that both the pure Diesel and 69% NG combustion processes produced two combustion peaks. The first combustion peak resulted from premixed Diesel combustion in the pure Diesel case and pilot Diesel combustion together with some combustion of the NG/air

mixture surrounding the pilot spray in the 69% NG case. Therefore, the first peak was larger in the 69% NG case than in the pure Diesel case. After the first peak, diffusion-controlled combustion became dominant in the pure Diesel case. However, another four distinct combustion modes were identified in the 69% NG case, as shown in Figure 4.1. The 69% NG case had a faster burning rate than pure Diesel. However, in the 95% NG case, the small quantity of pilot Diesel resulted in a smaller first combustion peak. Since less heat was released from Diesel combustion, the remaining NG burned in flame propagation mode rather than via chemical reaction-controlled bulk end gas autoignition. The combustion duration was longer in the 95% NG case than in the 69% NG case, resulting in less efficient combustion. The $CH_4$-Diesel cases generally behaved similarly to the 95% NG case. After the initial premixed combustion, the $CH_4$/air mixture burned in flame propagation mode because its burning rate was slower than the chemical reaction-controlled end gas autoignition in the 69% NG case. The rate of heat release traces also showed that the ignition delay in the NG-Diesel cases was shorter than in the $CH_4$-Diesel cases. Bourque et al. [114] also reported that ignition delay periods and flame speeds for typical pipeline natural gas compositions with small concentrations of heavier hydrocarbons (e.g. ethane, propane and butane) can be quite shorter compared with pure methane. The pressure traces shown in Figure 7.2 indicated that the combustion of 69% NG was more intense than that of pure Diesel, and produced higher peak pressures. However, both $CH_4$-Diesel cases (70% $CH_4$ and 81% $CH_4$) produced only slightly higher peak pressures than the pure Diesel case. Figure 7.4 shows that the dual-fuel cases produced higher overall HC and CO emissions than the pure Diesel cases due to the trapping of premixed gas/air mixture in the piston crevices. The $CH_4$-Diesel cases also produced higher HC emissions than the NG-Diesel cases, indicating that burning pure methane was more difficult than burning NG.

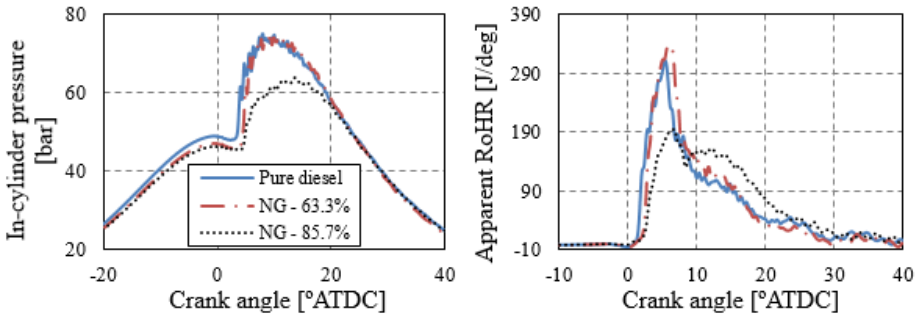


Figure 7.1: In-cylinder pressure and apparent heat release rate traces obtained from tests with pure Diesel and Diesel mixtures containing 63.3% and 87.5% NG at 6 bar BMEP

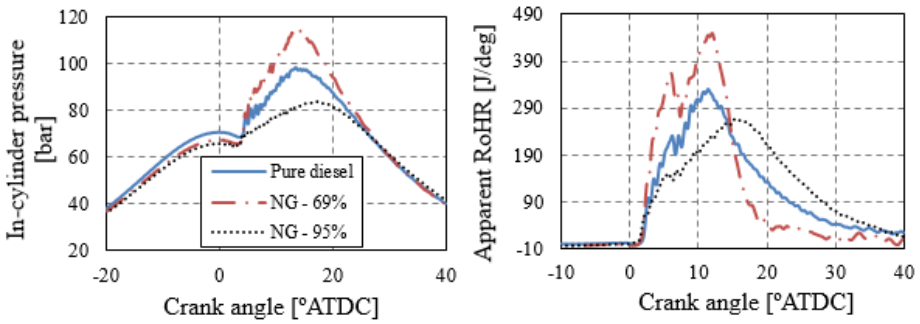


Figure 7.2: In-cylinder pressure and apparent heat release rate traces obtained from tests with pure Diesel and Diesel mixtures containing 69% and 95% NG at 12 bar BMEP

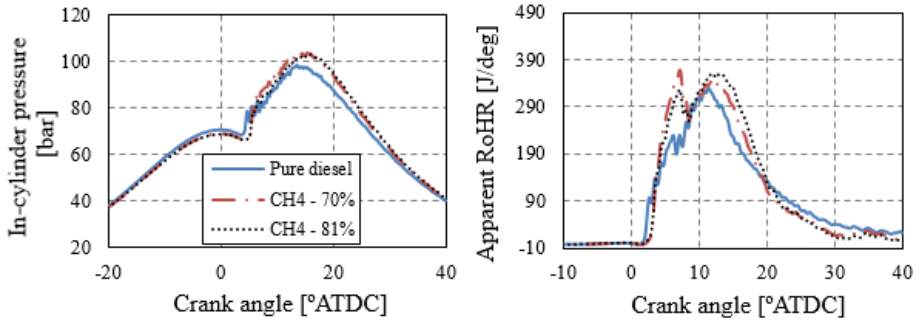


Figure 7.3: In-cylinder pressure and apparent heat release rate traces obtained from tests with pure Diesel and Diesel mixtures containing 70% NG and 81% $CH_4$ at 12 bar BMEP

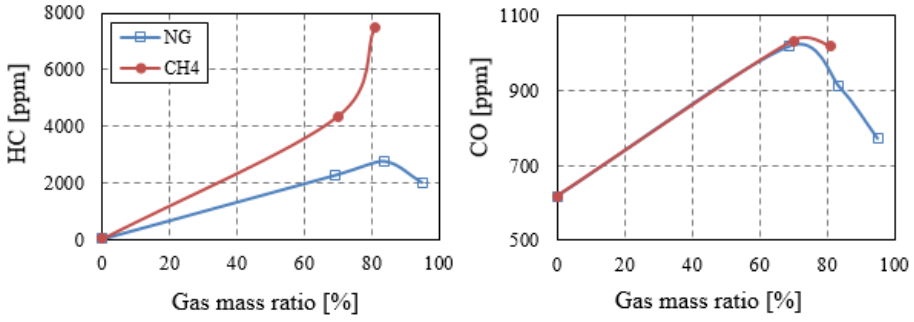


Figure 7.4: Unburned hydrocarbon and carbon monoxide emissions as functions of the gas mass ratio

It is also worth comparing pure Diesel and gas-Diesel combustion at similar mass ratios to examine the effects of the two gaseous fuels. The pressure and apparent RoHR traces for the pure Diesel, 69% NG, and 70% $CH_4$ cases are shown in Figure 7.5. The rate of heat release traces in the right-hand panel clearly show that the pure Diesel and 69% NG cases had very similar ignition delays, which were shorter than that for the 70% $CH_4$ case. Moreover, the NG/air mixture burned faster than the 70% $CH_4$/air mixture. It was therefore proposed that the two dual-fuel cases had different combustion modes. It seems that the main NG/air mixture (i.e. the fuel mixture burned after the first peak) initially burned in flame propagation mode after reaching the second peak but then mostly burned in the chemical reaction-controlled end gas autoignition mode. However, the main $CH_4$/air combustion process seemed to occur primarily via flame propagation, producing a lower heat release rate. Compared to the diffusion-controlled combustion seen in the pure Diesel case, the second combustion phase in the gas-Diesel case was more intense and produced higher peak pressures and temperatures, resulting in higher $NO_x$ emissions. The HC emissions for the 70% $CH_4$ case were around twice those for the 69% NG case, which was expected because pure $CH_4$ is comparatively difficult to burn. The AVL smoke meter was unable to detect any soot in either of the dual-fuel cases. The 69% NG case yielded the best equivalent brake specific fuel consumption (EBSFC) because its fast combustion resulted in the shortest combustion duration.

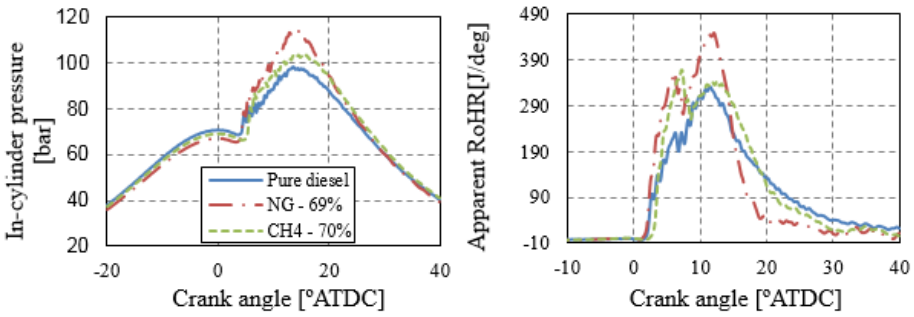


Figure 7.5: In-cylinder pressure and heat release rate traces obtained from tests with pure Diesel and Diesel mixtures with 69% NG and 70% $CH_4$ at 12 bar BMEP

Table 7.1: Emissions and EBSFC values for the cases shown in Figure 7.5

| Fuel | HC [ppm] | CO [ppm] | $NO_x$ [ppm] | Smoke number [-] | EBSFC [g/kWh] |
|---|---|---|---|---|---|
| Pure Diesel | 19 | 617 | 933 | 0.87 | 222.0 |
| NG 69% | 2252 | 1221 | 1568 | 0 | 211.5 |
| $CH_4$ 70% | 4348 | 1034 | 1333 | 0 | 216.1 |

## 7.2 Conventional gas-Diesel 3D model validation

The conventional gas-Diesel 3D model was described in Chapter 6, and details of its validation are presented in paper II. Three different cases (pure Diesel, NG-Diesel and $CH_4$-Diesel) were used to validate the 3D CFD dual-fuel model against experimental data at a load of 6 bar BMEP and 1500 rpm. Validation was performed by comparing the simulations' predictions of engine performance and emissions to the corresponding experimental data. The pure Diesel model adequately captured the main features of Diesel combustion, with ignition occurring at the tip of the fuel jet, followed by gradual flame propagation due to diffusion-controlled burning of the fuel/air mixture. The dual-fuel model also predicted the main characteristics of dual-fuel combustion including the presence of multiple-kernel flame propagation as shown in Figure 7.6. Engine performance was primarily characterized in terms of pressure traces and rate of heat release curves, and relatively good agreement between simulation and experiment was observed for all three cases. However, the ignition delays predicted by the simulations were consistently shorter than those observed experimentally. In addition, there were discrepancies between the predicted emissions and the experimental measurements for all three cases. These disagreements indicate that the models need to be further tuned by improving the dual-fuel combustion model and refining the chemical combustion mechanisms and other sub-models.

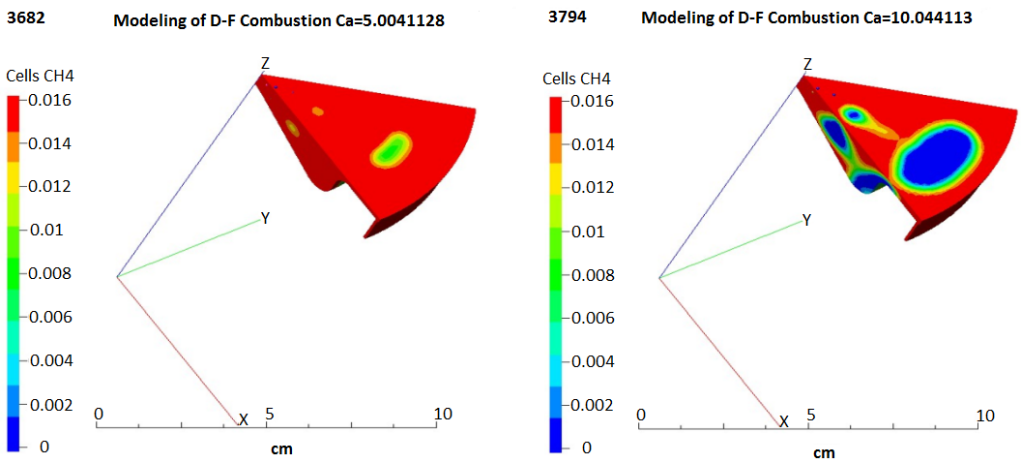


Figure 7.6: Methane concentration contours for NG-Diesel combustion

## 7.3 NG-Diesel RCCI combustion

Two studies focusing on NG-Diesel RCCI combustion were performed. Paper III reported a preliminary study on RCCI combustion that examined the effect of varying engine parameters such as the SOI, Diesel injection quantity, EGR rate, compression ratio (CR), engine load, and speed. Paper IV explored the effects of late IVC timings on NG-Diesel RCCI combustion.

### 7.3.1 Investigation of selected engine parameters' effects on RCCI combustion

Paper III presented experimental findings concerning the effects of selected engine parameters on NG-Diesel RCCI combustion. Characteristic experiments were performed at 9 bar BMEP and 1200 rpm, with a CR of 17. At a fixed natural gas substitution percentage (NGSP) of 67%, a sweep over the PI1 (pilot injection 1) SOI timing caused changes in the fuel mixture's stratification, which in turn affected the engine's performance and emissions as shown in Figure 7.7. Although the combustion phasing (CA50) was retarded by advancing the SOI, all cases with 42% EGR had a combustion phasing before TDC, which would increase the compression work and therefore reduce thermal efficiency. It thus seems that with an NGSP of 67%, changes in mixture stratification induced by varying the PI1 SOI can only influence combustion phasing to a very limited extent.

Another investigation was carried out to determine how the NGSP affects RCCI combustion and performance. NGSP was varied in two different ways: by varying the duration of PI2 (pilot injection 2) while fixing that

of PI1, and vice-versa. Figure 7.8 clearly shows that fixing the PI1 duration enabled the use of much lower NGSP values without harming performance and emissions than was possible when fixing the PI2 duration. The highest NGSP level examined in this work was 87.8%, which was the only case in which the combustion phasing was slightly after TDC. At this high level of gas substitution, the engine retained a high indicated thermal efficiency 52.9% with ultra-low soot emissions (0.005g/kWh), relatively low $NO_x$ (1.08g/kWh) emissions, and moderate levels of CO (2.23g/kWh) and HC (13g/kWh). Therefore, reducing fuel mixture's reactivity in this way offered an opportunity to improve combustion and emissions. Figure 7.9 shows that when the total Diesel injection duration was held constant, the engine's performance and emissions when the PI1 duration was set to 3.6 or 4.32 °CAD clearly differed from those seen when the PI2 duration was set to the same values. Table 7.2 shows that with the same total injection duration, the mixture's reactivities with varying PI1 were lower than cases with varying PI2. However, the CA50 and maximum PRR measurements suggest that varying PI1 made it possible to achieve more intense combustion than was observed with varying PI2. This was probably attributed to a reduction in mixing time between the first and second injections when varying PI1, which would increase fuel mixture stratification. Increased mixture stratification resulting from reduced mixing times has previously been reported by Hanson et al. [30].

Table 7.2: Injection duration and NGSP applied when testing the impact of varying the duration of PI1 and PI2

| Strategy | PI1 varied | | | | PI2 varied | | | | |
|---|---|---|---|---|---|---|---|---|---|
| Diesel injection duration 1 [°CA] | 2.74 | 2.88 | 3.60 | 4.32 | 2.88 | | | | |
| Diesel injection duration 2 [°CA] | 2.88 | | | | 2.16 | 2.52 | 2.88 | 3.60 | 4.32 |
| NGSP [%] | 80.1 | 78.4 | 71.5 | 63.4 | 87.7 | 83.7 | 78.4 | 67.0 | 58.9 |

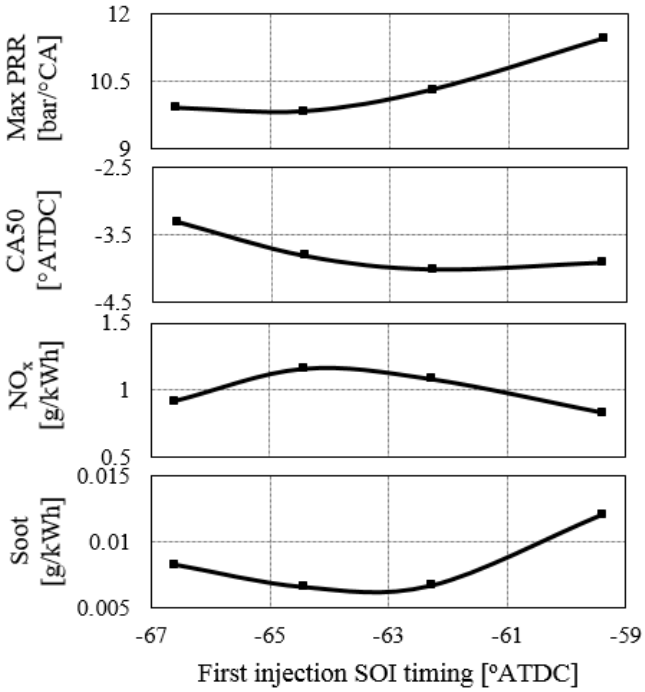


Figure 7.7: The influence of the PI1 SOI timing on performance and emissions

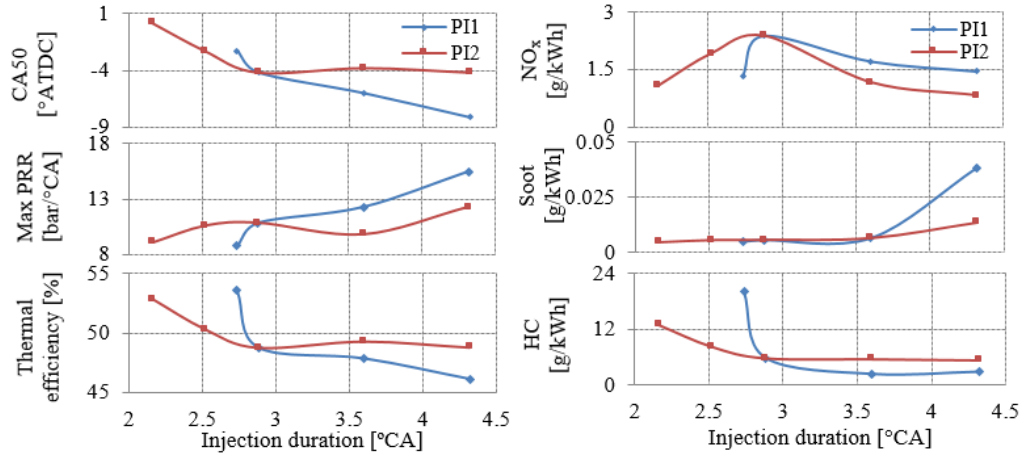


Figure 7.8: The influence of PI1 and PI2 duration on performance and emissions: the blue line represents PI2 held constant and PI1 varying; red line represents PI1 held constant and PI2 varying

The impact of the compression ratio (CR) on engine performance and emissions in RCCI combustion was also investigated by performing experiments using a piston with a reduced compression ratio of 14 and the engine's original piston, which had a compression ratio of 17. The maximum cylinder pressure tolerated by the engine limited the maximum load achievable at

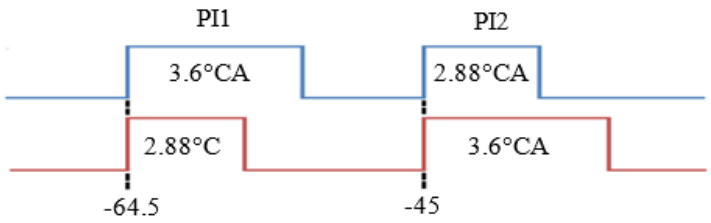


Figure 7.9: Diesel injection profiles for two test cases involving PI1 and PI2 durations of 3.6°CA

CR17 to 10 bar BMEP. Three loads (7, 9 and 10 bar BMEP) were tested at 1500 rpm with 42% EGR and an NGSP of 72% for CR values of 14 and 17. As shown in Figure 7.10, the combustion duration with CR17 was generally shorter than that with CR14. Consequently, the indicated thermal efficiency with CR 17 was higher than that with CR14 at 7 bar and 9 bar BMEP even though the combustion phasing was generally before TDC in the CR17 case. The decrease in indicated thermal efficiency at 10 bar BMEP for both CRs may have been due to a decrease in the specific heat ratio because the equivalence ratio increased with the load and there was more intensive heat transfer to the cylinder walls than in the low load cases. The rate of heat release rate curves for both CRs are shown in Figure 7.11. The peak rate of heat release at CR17 was greater than the corresponding value at CR14. The slopes of the ascending flank of the heat release rate curves changed part-way along their lengths for 7 & 9 bar BMEP at CR14 and 7 bar BMEP at CR17 because the combustion processes shifted from faster combustion controlled by kinetics to slower combustion controlled by flame propagation. This change in slope is absent in the other heat release rate curves, indicating that the premixed combustion in the other cases was mainly controlled by kinetics. Although the cases with CR14 seemingly had better combustion phasing than those with CR17, CR14 also seemed to produce a lower proportion of premixed combustion, which tends to reduce indicated thermal efficiency. Therefore, the CR17 piston was used in the subsequent NG-Diesel RCCI combustion study, and the effect of late valve closing was investigated in an attempt to improve combustion phasing and to increase the proportion of premixed combustion as well as the upper operating load limit.

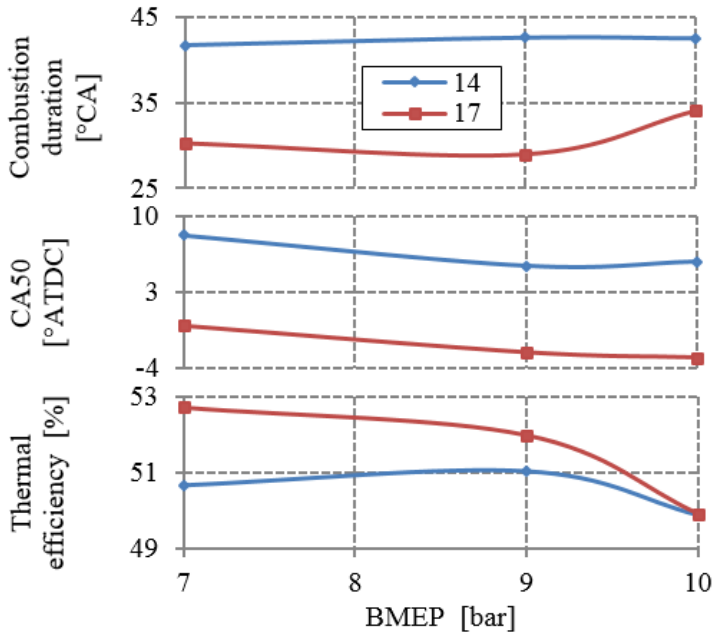


Figure 7.10: Engine performance at compression ratios of 14 and 17 under various load conditions

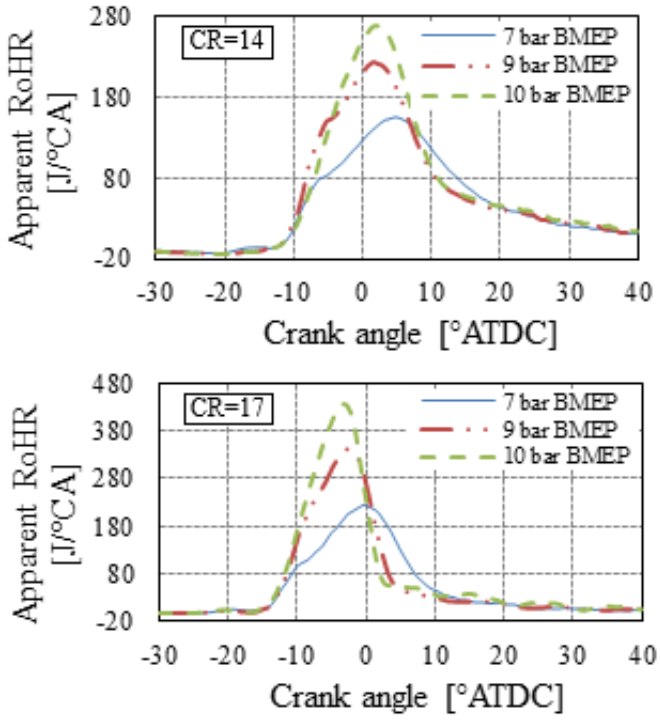


Figure 7.11: Rate of heat release traces for compression ratios of 14 and 17

### 7.3.2 Investigation into RCCI combustion with late inlet valve closing

A final study on NG-Diesel RCCI combustion was performed with a variable valve system to enable the use of different inlet valve closing timings (Paper IV). As mentioned before, the CR17 piston tested in the first NG-Diesel RCCI combustion study was also used in this study. Most of the characteristic investigations were conducted at 9 bar BMEP and 1200 rpm.

The impact of single and double Diesel injection strategies on NG-Diesel RCCI combustion was tested at various equivalence ratios with inlet valve closing at -124 °ATDC. The SOI values for the single and double strategies were -55 °ATDC and -53 & 0 °ATDC, respectively. The numerical model discussed in Section 6.1.2 was used to explore the combustion processes for both injection strategies at an equivalence ratio of 0.74. Although it was established that the model needs further tuning to address some discrepancies with reference data, the pressure and RoHR traces predicted by the simulations agreed reasonably well with the experimental results, as shown in Figure 7.12. This indicated that the model could be used to explain interesting combustion features on the basis of temperature and equivalence contours. The temperature contour plots in Figure 7.13 show that the single injection strategy produced more high temperature zones than the double injection strategy at various crank angles. This indicates that the single injection strategy yielded more intense and faster combustion than the double injection strategy. Figure 7.13 also shows that high temperature combustion began at -4 and -3 °ATDC for the single and double injection cases, respectively. The total quantity of injected Diesel was the same for both injection strategies at the same equivalence ratio. However, because the second injection in the double injection strategy started at 0 °ATDC, the amount of Diesel present in the cylinder when the main combustion process began was larger in the single injection cases than in the double injection cases. The upper image in Figure 7.14 shows that the mixtures formed with the single injection strategy were more reactive than those for the double injection strategy. The single injection strategy thus produced more reactive fuel mixtures than the double injection strategy, which led to higher cylinder pressure and temperatures with single injection strategy. This generally resulted in higher $NO_x$ emissions and more advanced combustion phasing (CA50) in the single injection case at various equivalence ratios, as shown in Figure 7.15. The high soot emissions observed in the double injection cases (see Figure 7.15) were attributed to the late injection near TDC, which would form locally rich regions causing soot formation.

Such a locally rich region can be seen in Figure 7.14 at 3 °ATDC. As for the indicated thermal efficiency, there's no strong dependency on injection strategy. The difference between the two injection strategies at an equivalence ratio of 0.71 was due to slight differences in the NG energy substitution percentage. This made the total fuel energy in the single injection case slightly greater than in the double injection case.

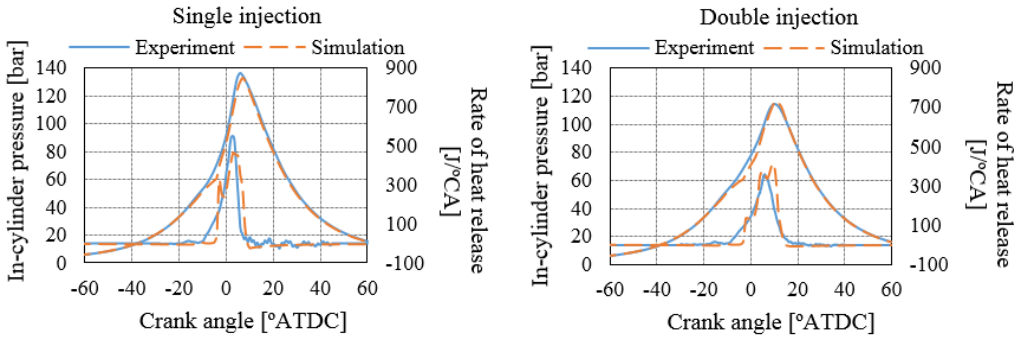


Figure 7.12: In-cylinder pressure and RoHR traces from simulations and experiments for single and double Diesel injection strategies at an equivalence ratio of 0.74

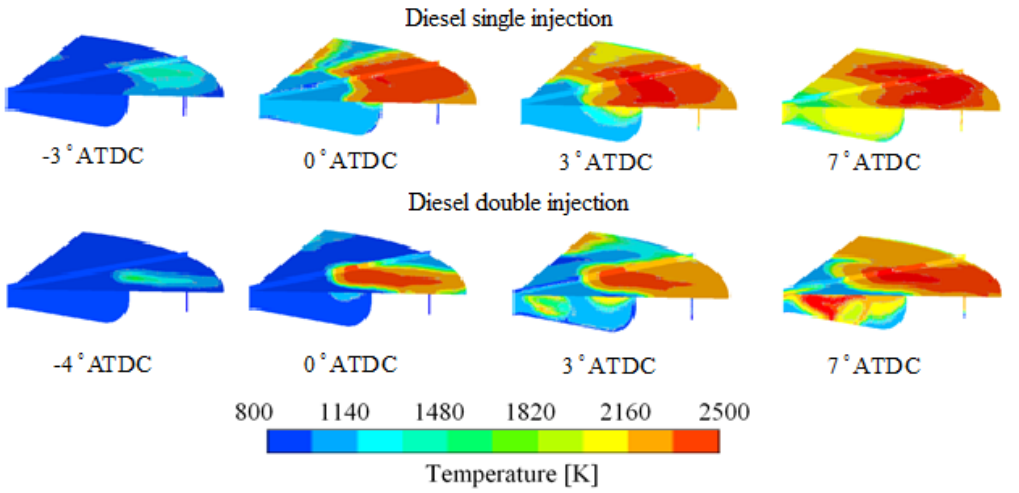


Figure 7.13: Cut plane temperature contour plots for various crank angles and a global equivalence ratio of 0.74

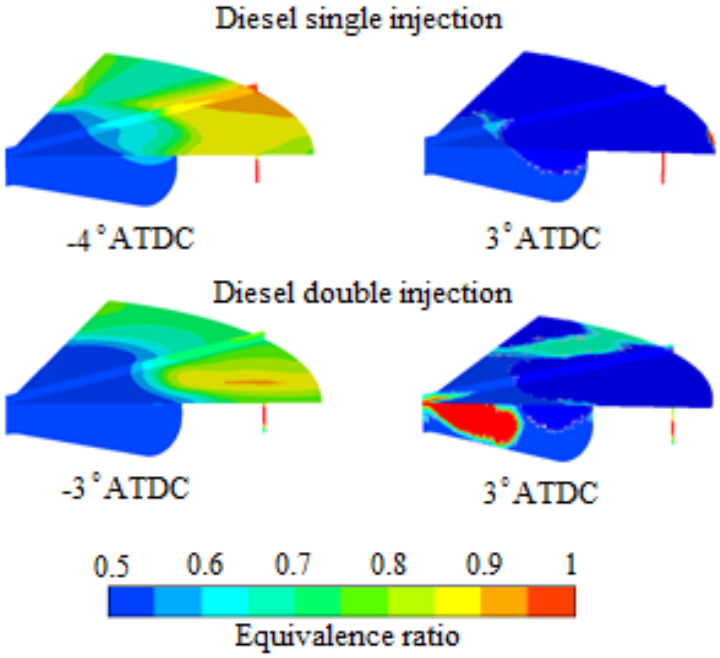


Figure 7.14: Cut plane equivalence ratio contour plots for two crank angles and a global equivalence ratio of 0.74

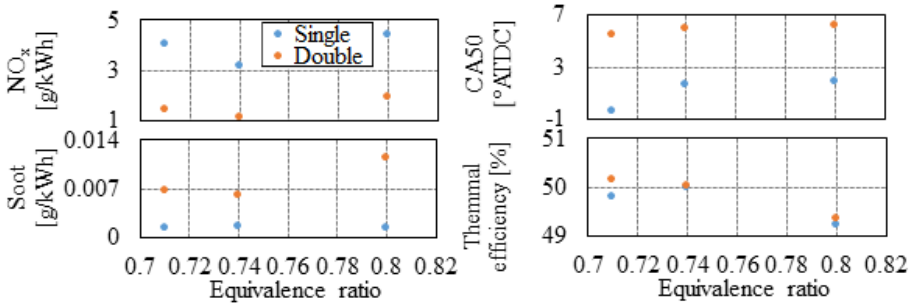


Figure 7.15: Emissions and performance for single and double Diesel injection strategies

In the first NG-Diesel RCCI study (Section 7.3.1), it proved somewhat difficult to control the combustion phasing at CR17 since most cases had combustion phasing before TDC. To overcome this issue, combustion phasings of CA50 = 0, 2, 6 and 9.5 °ATDC were tested at various IVC timings. These different CA50 phasings were maintained by using a double injection strategy and adjusting parameters such as the equivalence ratio, NGSP, and EGR levels while operating the engine at 9 bar BMEP and 1200 rpm. Figure 7.16 shows the engine out emissions and performance observed at different CA50 and IVC timings. $NO_x$ emissions generally increased with the retardation of IVC timing except at a combustion phasing of CA50=9.5

°ATDC. This trend contradicted the expectation that a late IVC with a low effective compression ratio would yield low $NO_x$ emissions, and was attributed to the manipulation of the equivalence ratio and EGR to maintain the desired CA50 phasing. For instance, at an IVC of -124 °ATDC, a slightly richer mixture was used than in the other cases to maintain a constant CA50 phasing. No data on soot emissions (0.0049 - 0.0149 g/kWh) are presented because they did not vary in any consistent way with either the CA50 phasing or the IVC. In addition, CO emissions were almost constant, but $CH_4$ emissions decreased as the IVC timing was retarded. Emissions of both these species increased with the retardation of the combustion phasing, and this behavior explains much of the observed trend in the combustion efficiency. Acceptable combustion stability was achieved at all test points because the CoV in IMEP was consistently below 3%. The equivalent break specific fuel consumption (EBSFC) at combustion phasing 9.5 °ATDC was higher than that of other combustion phasings due to the lowest combustion efficiency at this combustion phasing. For all other phasings, retarding the IVC timing generally increased EBSFC. The best performance in terms of fuel economy and $NO_x$ emissions was achieved with an IVC timing of -143 °ATDC and a combustion phasing of 6 °ATDC.

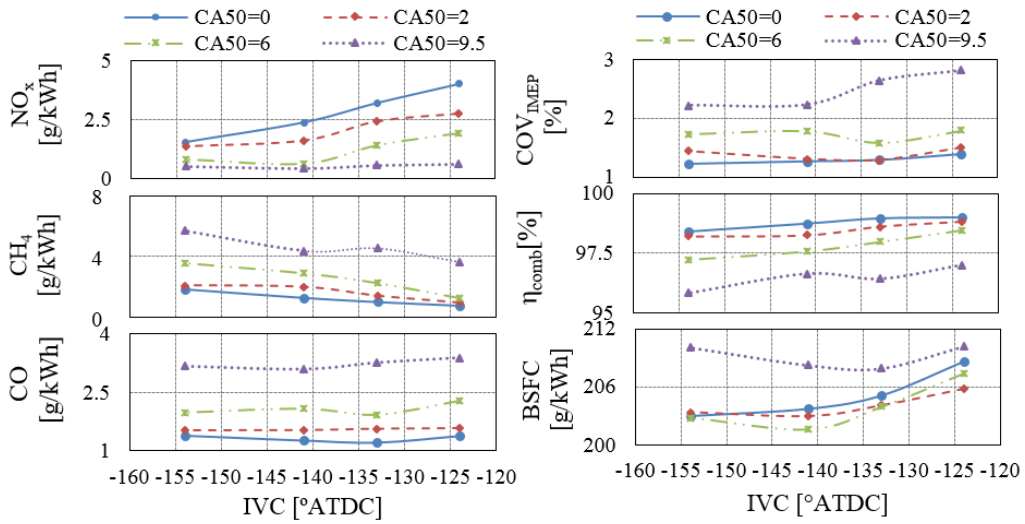


Figure 7.16: Engine-out emissions and performance at different CA50 values and IVC timings

To obtain an overview of RCCI combustion at various engine speed and loads, NG-Diesel RCCI experiments were performed with an IVC of -124 °ATDC using a double Diesel injection strategy. The performance and emissions of NG-Diesel RCCI combustion were compared with the conventional

Diesel combustion, which were conducted with an IVC of -180 °ATDC, SOI at -6 °ATDC, and an injection pressure of 2000 bar. Figure 7.17 shows the relative reductions (expressed as percentages) in EBSFC, maximum pressure rise rate (PRR), and emissions of $NO_x$ and soot obtained when using RCCI combustion rather than conventional Diesel combustion under the test conditions. RCCI cases achieved lower EBSFC values than conventional Diesel cases at many different loads and engine speeds, with an improvement of almost 11% at a load of 11 bar BMEP and a speed of 1800 rpm. The engine speed had a greater effect on the relative improvement in fuel economy than did the load. The maximum PRR measurements indicated that conventional Diesel combustion was generally noisier than RCCI. However, the relative reductions in the maximum PRR were more strongly dependent on the load than the engine speed, and decreased as the load increased when the engine speed was kept constant. Conversely, the relative reductions in $NO_x$ and soot emissions exhibited no clear dependence on either the load or the engine speed. However, RCCI cases produced vastly lower soot emissions than conventional Diesel cases over a very wide range of loads and engine speeds. Although the $NO_x$ levels produced by RCCI were somewhat higher than for conventional Diesel combustion at certain loads and speeds, the data shown in Figure 7.18 demonstrate that the absolute $NO_x$ levels produced during RCCI combustion were relatively low. The results presented in paper IV (especially those relating to the use of late IVC at different equivalence ratios and engine speeds) suggest that there is considerable scope for tuning the RCCI combustion process to further reduce $NO_x$ emissions without excessively harming other important aspects of performance.

It was noted that the maximum tolerable load for RCCI case at CR17 was 10 bar BMEP in the first NG-Diesel study (Section 7.3.1). Subsequent experiments with late IVC revealed operating points that permitted substantial RCCI load extension: a maximum tolerable load of 14 bar BMEP was achieved using RCCI with a double injection strategy at 1500 rpm and CA50 5.5 °ATDC with an IVC timing of -124 °ATDC. Unfortunately, higher loads could not be tested because the resulting peak pressures could have exceeded the engine's maximum cylinder pressure of 180 bar. Figure 7.19 shows cylinder pressure and heat release rate traces for the highest safe load. The combustion duration was very short, and the peak pressure occurred at 11°ATDC. The indicated thermal efficiency under these conditions was 50 %, while the levels of $NO_x$ and soot were 1.93 and 0.048 g/kWh, respectively. The use of late IVC timing thus increased the maximum operating load by up to 40%.

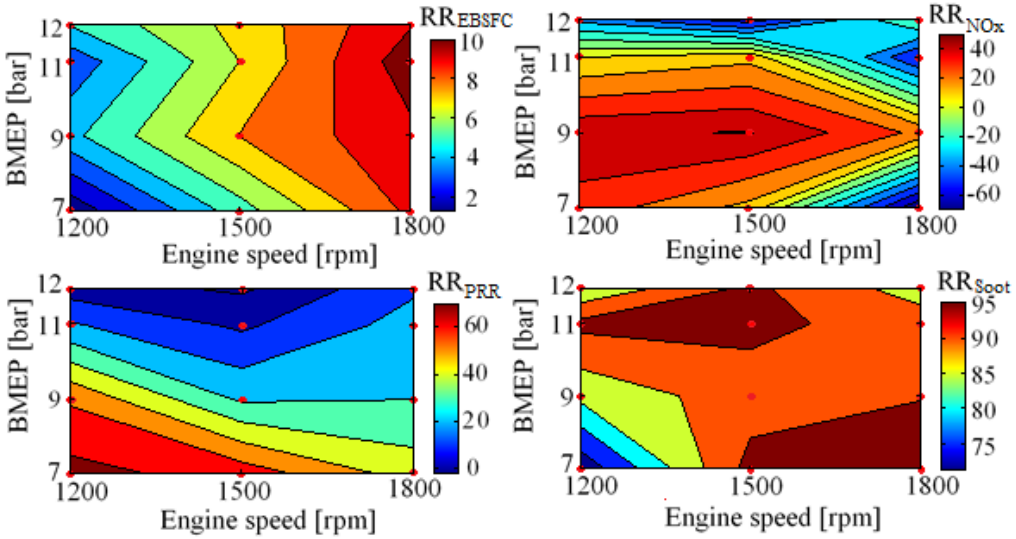


Figure 7.17: Relative reductions in selected parameters when using NG-Diesel RCCI combustion instead of conventional Diesel combustion [%]

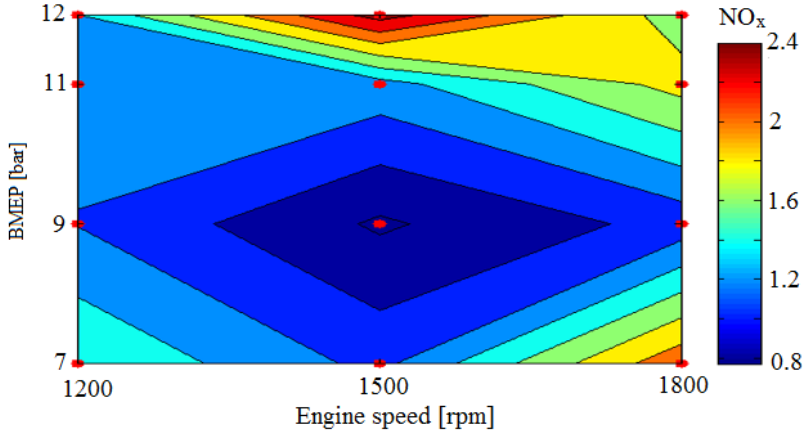


Figure 7.18: $NO_x$ emissions for NG-Diesel RCCI at various engine speeds and loads

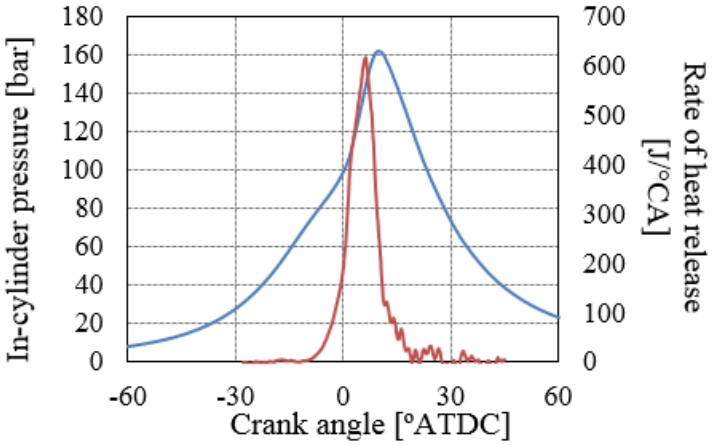


Figure 7.19: The pressure and rate of heat release traces observed when using RCCI with late IVC at 14 bar BMEP

## 7.4 Methanol-Diesel RCCI combustion

Another alternative fuel tested during the experimental campaign was methanol. The main purpose of Paper V was to investigate methanol-Diesel RCCI combustion with three different methanol injection configurations: port injection into the intake manifold; direct injection during the intake stroke (DI_E) and direct injection during the compression stroke (DI_L). Characteristic investigations focusing on variables such as the Diesel SOI, Diesel injection duration ratio, and methanol substitution percentage (MSP) were carried out at a constant engine speed and load of 1500 rpm and 5 bar IMEP, with a constant intake temperature of 60°C. The MSP used in the DI_L configuration (∼53%) was lower than in the port and DI_E configurations (∼66%) for the sweeps of Diesel SOI and duration ratio. The reason for this was because, for the last rebuild to DI_L configuration, it couldn't run stably if the same settings as were used as for the port and DI_E configurations.

In-cylinder pressure and gross rate of heat release traces for a PI1 SOI of -48 °ATDC and a PI2 SOI of -15 °ATDC with the three different configurations are shown in Figure 7.20. The combustion processes for the DI_E and port configurations were very similar and differed markedly from that for the DI_L configuration. Kokjohn [115] showed that at very lean equivalence ratios, flame propagation contributes little to combustion. The methanol/air global equivalence ratios used in this investigation were 0.22 for the DI_L configuration and 0.25 for the DI_E and port configurations, so combustion under all three configurations was primarily kinetically-controlled. All three configurations generated two high temperature heat release (HTHR) peaks. The DI_L configuration used a larger Diesel injection than the other two configurations, and therefore formed more reactive mixtures. Consequently, its HTHR started much earlier and it burned more rapidly until several degrees before TDC. After that, the mixture in the DI_L configuration burned more slowly and had a longer tail than those for the other two configurations. The lower rate for DI_L after TDC was possibly attributed to lower kinetic reaction rates, and the long tail of its RoHR trace was attributed to mixing-controlled combustion resulting from the larger Diesel injection.

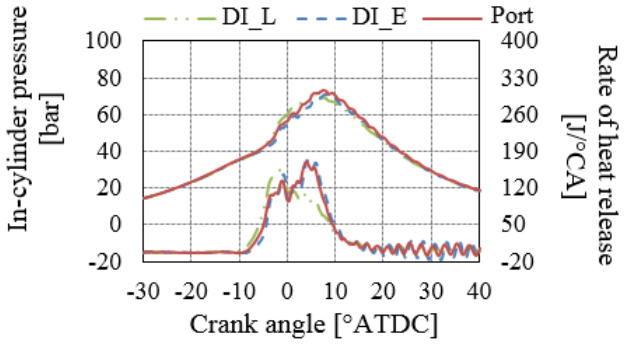


Figure 7.20: In-cylinder pressure and gross RoHR traces at PI1 SOI -48 °ATDC and PI2 SOI -15 °ATDC for three methanol injection configurations

Experiments using different Diesel SOI timings (PI1 and PI2) and Diesel duration ratios revealed that all three of these parameters had lower and upper limits resulting from either too early combustion phasing (CA50<0) or unstable combustion. Figure 7.21 shows different performance and emissions over a sweep of the Diesel PI1 SOI from -50 to -34 °ATDC for the three methanol injection configurations. The highest methanol emissions were observed for the DI_L configuration, indicating that larger portion of methanol was not in the flammable region compared to DI_E and port configurations due to the use of a leaner methanol/air mixture. This is partly why the DI_L configuration achieved the lowest combustion efficiencies. The port configuration had the highest net indicated thermal efficiency, followed by the DI_E configuration and then the DI_L configuration. This trend was largely due to the differences in combustion efficiency between the three configurations. Additionally, in the DI_L configuration, the combustion during the compression stroke was more advanced than in the other configurations, meaning that the piston had to do more work on the cylinder gases, the combustion rate after TDC was lower, and the tail of RoHR trace was longer. Therefore, the DI_L configuration extracted less useful work from the fuel mixture. The PI1 SOI had a strong influence on the combustion phasing (CA50) at values of up to -43 °ATDC for all three configurations. $NO_x$, and CO emissions correlated well with the combustion phasing: more obvious increasing or decreasing trend till PI1 SOI -43 °ATDC. The emissions after PI1 SOI -43 °ATDC were almost constant. The results for the Diesel PI2 SOI sweep shown in Figure 7.22 demonstrate that the port configuration had a much narrower PI2 SOI span than the DI_L and DI_E configurations, which was not seen in the PI1 sweep. The net indicated thermal efficiency exhibited a similar trend to that seen in the PI1 SOI studies: it was highest for the port configuration, followed by the DI_E configuration and then the DI_L configuration. Since both HC and $NO_x$ emissions generally exhibited

clear and strong increasing or decreasing trends during the Diesel PI2 SOI sweep, adjusting the PI2 SOI appears to be a more efficient way of tuning mixture stratification to improve combustion than adjusting the PI1 SOI.

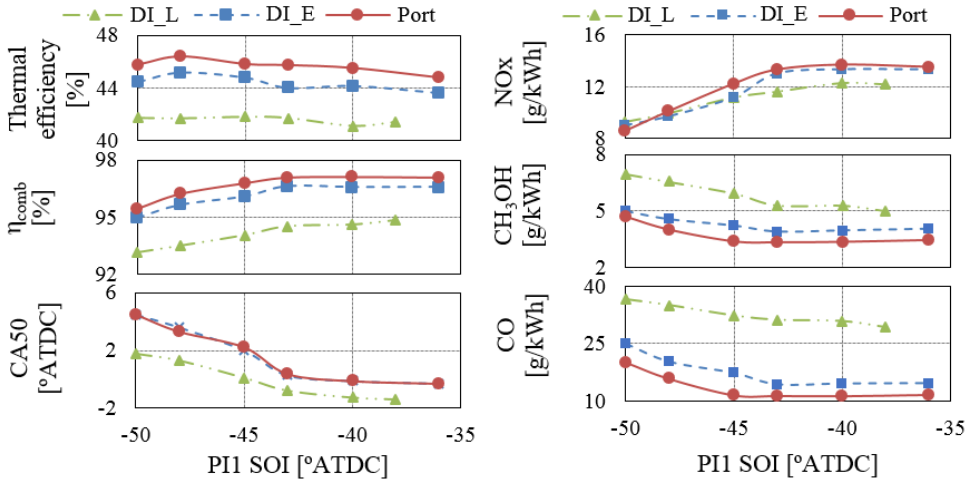


Figure 7.21: Effect of PI1 SOI on emissions and performance during methanol-Diesel RCCI combustion

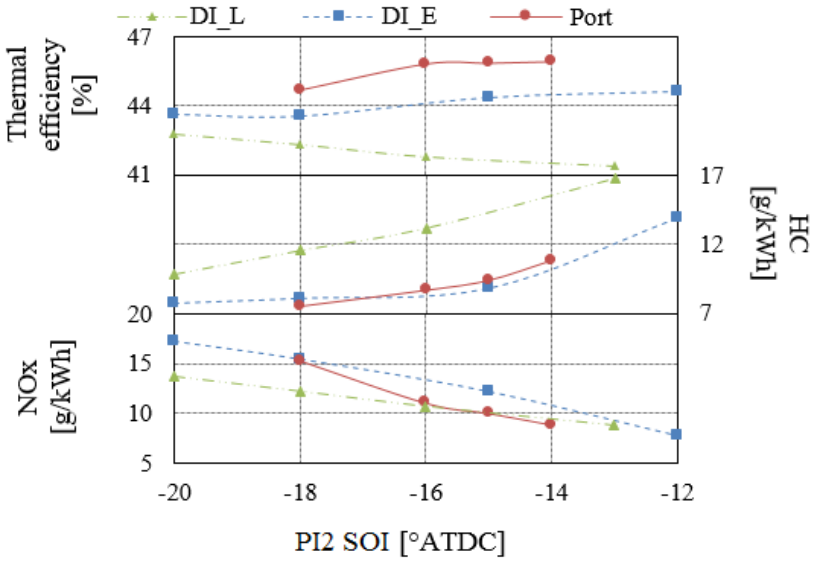


Figure 7.22: Effect of PI2 SOI on thermal efficiency and emissions during methanol-Diesel RCCI combustion

The engine's performance and emissions were also examined at loads of 5, 8, 10 and 12 bar IMEP using the port and DI_L methanol configurations and a reference Diesel system, as shown in Figure 7.23. There were no significant

differences between the three configurations with respect to net indicated thermal efficiency or HC and CO emissions. However, the use of methanol instead of Diesel as the main fuel in the port and DI_L configurations reduced greenhouse gas emissions relative to the pure Diesel case at all tested loads due to methanol's low C/H ratio. The port configuration satisfied the Euro 6 requirements for NOx and soot emissions at 12 bar IMEP, but the DI_L and Diesel configurations did not. Overall, direct methanol injection in the compression stroke did not yield any detectable benefits over the load sweep relative to the port configuration. Since this work was the first experimental test of these methanol injection configurations, no optimization has been done; optimization of the system is expected to improve its fuel economy and emissions.

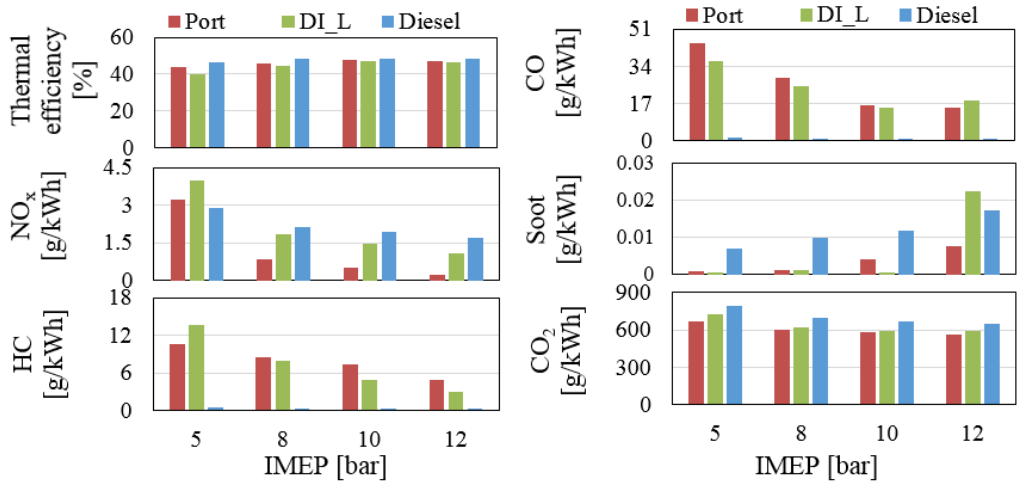


Figure 7.23: Engine efficiency and emissions at different loads

# Chapter 8

# Conclusion

This chapter summarizes the work included in the thesis. The first part of the thesis work involved studying conventional gas-Diesel dual-fuel combustion using the Volvo D12C single cylinder heavy-duty engine. Experimental data generated during this work were used to validate a 3D dual-fuel combustion model developed at Chalmers. The second part of the thesis work examined the use of Reactivity Controlled Compression Ignition (RCCI) combustion with alternative fuels in Diesel engines, focusing primarily on NG-Diesel and methanol-Diesel RCCI combustion. The effects of various engine and fuel parameters were studied to improve the understanding of RCCI combustion.

The results obtained for conventional gas-Diesel dual-fuel combustion were consistent with previous reports: dual-fuel operation yielded high overall unburned HC and CO emissions, and improved engine performance and emissions markedly under high load conditions but less so under low load conditions. However, our results contradicted an earlier report [116] with respect to the influence of the NG supplement ratio on the in-cylinder pressure and combustion duration. It seems that the results showed some dependency on the experimental setup and other engine parameters (e.g. the intake temperature, pressure, injection pressure, and equivalence ratio). Comparisons of NG-Diesel and $CH_4$-Diesel dual-fuel combustion revealed that cases with NG had shorter ignition delays. Moreover, at similar mass ratios, NG-Diesel combustion yielded shorter combustion durations and lower HC emissions than $CH_4$-Diesel combustion. This suggests that NG, which contains other compounds such as ethane, propane, and butane, makes the fuel mixture more reactive than pure methane.

The 3D dual-fuel combustion model developed at Chalmers was validated against the experimental data obtained in this work. The dual-fuel com-

bustion model captured the main characteristics of both pure Diesel and gas-Diesel dual-fuel combustion. It also achieved reasonably good agreement with experiment in terms of engine performance. However, there were some discrepancies between the experiments and simulations, particularly regarding the ignition delay and emissions. These discrepancies indicate that the model should be further tuned and refined, focusing on aspects of the chemical mechanisms and other sub-models.

The preliminary study of NG-Diesel RCCI combustion indicated that for most test cases at an EGR rate of 42% and a compression ratio (CR) of 17, the combustion phasing (CA50) occurred before TDC. At a high natural gas substitution percentage (NGSP) of around 84%, the combustion phasing could be slightly after TDC, which resulted in high indicated thermal efficiency of around 53%. To improve the combustion phasing, two parameters were varied - the EGR rate and the compression ratio. Increasing the EGR rate from 42% to 51% allowed the combustion phasing to be set to a more suitable value. The indicated thermal efficiency with an EGR rate of EGR 51% and an NGSP of 75.8% was about 2% higher than that achieved with an EGR rate of 42% and an NGSP of 82.4%. Using a lower compression ratio of 14 (referred to as CR14) at different loads also improved the combustion phasing relative to that achieved at CR17. However, combustion was slower at CR14, leading to longer combustion durations and lower thermal efficiencies, especially at loads of 7 and 9 bar BMEP. Due to limitations on the engine's maximum cylinder pressure, the highest load that could be tested at CR17 was 10 bar BMEP. Overall, these results indicate that further research is needed to find a way of achieving desirable combustion phasing together with high indicated thermal efficiencies and a high operational load limit when using NG-Diesel RCCI combustion.

Another study on NG-Diesel RCCI combustion was conducted focusing primarily on evaluating the effects of variable inlet valve closing timings on engine performance and emissions. Late inlet valve closing (IVC) extended the viable range of operating loads for RCCI combustion, increasing the maximum operating load by up to 40%. In addition, it was shown that a double Diesel injection strategy can be used to reduce the intensity of combustion and control combustion phasing more effectively than is possible with a single Diesel injection strategy. By selecting an appropriate combination of late IVC, EGR rate, equivalence ratio, and NGSP, one can selectively impose different combustion phasings. A combustion phasing of 6 °ATDC with IVC at -143°ATDC was found to be optimal with respect to fuel economy while maintaining acceptably low $NO_x$ emissions. Moreover,

indicated thermal efficiencies above 50% were achieved at various equivalence ratios and IVC timings. The $NO_x$ and soot emissions satisfied the Euro 6 requirements at the lowest tested equivalence ratio (0.64) when using a retarded inlet valve closing timing of -133 °ATDC. RCCI combustion offered better fuel economy than conventional Diesel combustion over a wide range of loads: the improvements in fuel combustion were as large as 11% in some cases, and tended to increase with the engine speed. The 3D CFD studies were also performed to clarify the details of NG-Diesel RCCI combustion. Although there's still some discrepancies between the simulations and the experimental data, the two were in reasonably good agreement, meaning that the simulation results could be used to explain aspects of the combustion process in terms of temperature profiles and equivalence ratio contours.

The final study of the thesis focused on methanol-Diesel RCCI combustion, and revealed that the DI_E and port configurations had very similar combustion patterns that differed markedly from those for the DI_L configuration. In all three configurations, there were clear lower and upper limits on the Diesel PI1 and PI2 SOI timings and the PI2/PI1 duration ratio resulting from the need to avoid overly early combustion phasings and unstable combustion. The PI2 SOI and PI2/PI1 duration ratio were identified as more effective parameters than the pilot SOI for the purposes of tuning mixture stratification to improve combustion. The DI_L configuration consistently yielded lower net indicated thermal efficiencies and higher emissions of HC and CO than the port and DI_E configurations because it had lower combustion efficiencies. The influence of the methanol injection pressure and methanol substitution percentage (MSP) was also investigated for the DI_L configuration, revealing that the combustion process was relatively insensitive to the methanol injection pressure but was adversely affected by increasing the methanol substitution percentage (MSP). The use of methanol instead of Diesel as the main fuel in the port and DI_L configurations reduced greenhouse gas emissions relative to the pure Diesel cases at all tested loads due to methanol's low C/H ratio. The port configuration satisfied the Euro 6 requirements for $NO_x$ and soot emissions at 12 bar IMEP, but the DI_L and Diesel configurations did not. Although these initial experiments using methanol direct injection prototypes didn't reduce emissions of HC and CO compared to port injection of methanol, further optimization of methanol direct injection systems using proper spray targeting and better fuel distribution are expected to improve both fuel economy and emissions.

# Chapter 9

# Future Work

The studies on dual-fuel RCCI combustion presented in this thesis have increased our understanding of this low temperature combustion regime and its sensitivity to different engine parameters. The next step in dual-fuel RCCI research should be to optimize RCCI combustion with the aim of improving its fuel economy and emissions profile to comply with increasingly strict emissions standards.

All RCCI studies reported to date have been performed using engine hardware designed for conventional Diesel combustion. Since the high-octane fuels such as NG/methanol were injected early during the intake stroke and formed a premixed fuel/air mixture in the cylinder, the use of bowl-shaped pistons and large piston crevice volumes increased the HC and CO emissions of RCCI combustion. A useful next step would therefore be to test new piston shapes designed specifically for RCCI combustion to reduce HC and CO emissions. Although mixture stratification and reactivity can be used to control the combustion phasing in RCCI, the bulk of the combustion occurs under kinetically-controlled conditions, which presents challenges at high load condition resulting from the maximum cylinder pressure limitation at high compression ratio. To enable RCCI operation at high loads, it would be desirable to introduce either a pistons designed for lower compression ratios or new crankshafts that can withstand higher maximum cylinder pressures.

While this thesis presents some 3D simulation work on RCCI combustion, there are still some disagreements between simulations and experiments relating to ignition delays and emissions. If the 3D CFD model were improved such that there was better agreement between simulations and experiments, it could be used to understand RCCI combustion physics and aspects of combustion such as the flame temperature and the formation of various

emissions. Moreover, it would be possible to simulate different kinds of engine hardware, facilitating the design of hardware optimized for RCCI. Finally, it would be possible to use 3D simulations to develop optimized control strategies to overcome the difficulties of controlling the combustion phasing and the high pressure rise rate currently associated with RCCI. In general, simulations are powerful tools for acquiring large amounts of useful information inexpensively.

High levels of unburned HC and CO emissions are common issues in RCCI combustion due to low cylinder wall temperatures and the trapping of high-octane fuel in crevices. The direct injection of high octane fuel into the cylinder has the potential to reduce these emissions, especially from crevices, by proper spray targeting and a better fuel distribution in the cylinder. Although the first trial using direct methanol injection did not yield any reductions in HC and CO emissions reduction compared to port injection, we believe that further optimization of the system will yield improvements in both fuel economy and emissions. Finally, since we have already studied port-injected NG RCCI combustion, it would be worth exploring direct-injected NG/biogas RCCI combustion.

# Chapter 10

# Summary of Papers

This chapter provides brief summaries of the papers included in the thesis.

## Paper I

### Effects of Natural Gas Percentage on Performance and Emissions of a Natural Gas/Diesel Dual-Fuel Engine

*Zhiqin Jia and Ingemar Denbratt*

The influence of the NG supplement ratio on NG/Diesel combustion was investigated at loads of 6 and 12 bar BMEP. In the low load case (6 bar BMEP), NG-Diesel combustion did not show favorable performance or emissions compared to pure Diesel combustion. Since the amount of Diesel needed at this load in the pure Diesel case was low, the Diesel was already well premixed with air during the ignition delay time. Therefore, dual-fuel combustion provided few advantages in the low load case. Further increasing the NG supplement ratio was expected to deteriorate the combustion and result in slow combustion, further increasing unburned HC emissions. In the intermediate load case (12 bar BMEP), increasing the NG supplement ratio beyond a certain level reduced the combustion duration. This fast combustion resulted in a higher in-cylinder pressure than in the pure Diesel case. This finding differs from a previous report [116] in which dual-fuel operation was found to produce a lower in-cylinder peak pressure and a longer combustion duration than pure Diesel combustion. Further increasing the NG supplement ratio deteriorated combustion because the quantity of Diesel used was too small to provide a good ignition source.

Author's contribution: ZJ performed the experiments together with Dr. Gjirja, post-processed the data, and wrote the article. Prof. Denbratt gave

support in experimental planning and paper writing.

## Paper II

### Validation of a Dual-Fuel Combustion Model for Heavy Duty Diesel Engines

*Zhiqin Jia, Valeri Golovitchev and Ingemar Denbratt*

The 3D CFD dual-fuel model was validated against experimental data for three different cases (pure Diesel, NG-Diesel and Methane-Diesel) at a load of 6 bar BMEP. Comparisons between simulation and experiment were carried out in terms of engine performance and emissions. The pure Diesel model adequately captured the main features of Diesel combustion, with ignition occurring at the tip of the fuel jet, followed by gradual flame propagation due to burning of the diffusion controlled fuel-air mixture. The dual-fuel model also predicted the main characteristics of dual-fuel combustion including the presence of multiple-kernel flame propagation. With respect to engine performance (characterized primarily in terms of pressure traces and rate of heat release plots), relatively good agreement between simulation and experiment was achieved for all three cases. However, the simulations consistently predicted a shorter ignition delay than was observed experimentally. Discrepancies were also observed between the emissions predicted by the simulations and the experimental results in all three cases. These disagreements indicate that the models need to be further tuned by improving the dual-fuel combustion model and refining the chemical combustion mechanisms and other sub-models.

Author's contribution: The 3D dual-fuel combustion model was developed by Dr. Golovitchev. ZJ provided the experimental data, used the 3D dual-fuel combustion model to conduct numerical work, and wrote the article. Prof. Denbratt and Dr. Golovitchev gave support in simulation and paper writing.

## Paper III

### Experimental Investigation of Natural Gas-Diesel Dual-Fuel RCCI in a Heavy-Duty Engine

*Zhiqin Jia and Ingemar Denbratt*

This paper reported a preliminary study of engine performance and emissions when using RCCI combustion. Different parameters such as the SOI, Diesel quantity, EGR, compression ratio (CR), engine load, and speed were investigated. By varying the SOI and Diesel quantity, it was found that the indicated thermal efficiency for all RCCI cases was higher than that obtained with pure Diesel when parameters such as the intake pressure, temperature, and EGR level were kept constant. Some of these RCCI cases yielded indicated thermal efficiencies above 50%. Soot emissions for the RCCI cases were quite low compared to the pure Diesel cases. However, $NO_x$ emissions were slightly higher than for pure Diesel.

Author's contribution: ZJ performed the experiments together with Dr. Gjirja and Dr. Benham, post-processed the data, and wrote the article. Prof. Denbratt gave support in experimental planning and paper writing.

## Paper IV

### Effect of Late Inlet Valve Closing on NG-Diesel RCCI Combustion in a Heavy Duty Engine

*Zhiqin Jia and Ingemar Denbratt*

The purpose of this study was to investigate the effect of late inlet valve closing (IVC) on NG-Diesel RCCI combustion in a single cylinder heavy-duty Diesel engine. The experiments were conducted at different IVC timings (-154, -141, -133, -124 and -111 °ATDC) and engine speeds (1200, 1500 and 1800 rpm). Indicated thermal efficiencies above 50% were achieved in most cases with various late inlet valve closing timings. Moreover, ultra-low $NO_x$ and soot emissions were observed at the lowest tested equivalence ratio (0.64) with retarded inlet valve closing timing (-133°ATDC) at 1200 rpm. The impact of inlet valve closing timing on the indicated thermal efficiency was stronger at 1200 rpm than at 1500 and 1800 rpm. Additionally, the use of late inlet valve closing increased the engine's maximum operational load by 40% compared to that reported in Paper III.

Author's contribution: ZJ performed the experiments together with Dr. Benham, post-processed the data, and wrote the article. Prof. Denbratt gave support in experimental planning and paper writing.

## Paper V

### Experimental Investigation into the Combustion Characteristics of a Methanol-Diesel Heavy Duty Engine Operated in RCCI Mode

*Zhiqin Jia and Ingemar Denbratt*

This study examined combustion in a dual-fuel methanol-Diesel heavy duty engine using three different methanol injection configurations: port injection into the intake manifold; direct injection during the intake stroke (DI_E), and direct injection during the compression stroke (DI_L). The engine used in the study was an AVL single cylinder heavy-duty engine with a displacement volume of 2.13L that was designed to mimic the Volvo Powertrain D13 engine. Characteristic investigations were conducted at a constant engine speed of 1500 rpm, 5 bar IMEP, and an intake temperature of 60°C. The DI_L configuration achieved lower net indicated thermal efficiencies and higher emissions of HC and CO than the other two methanol injection configurations. The influence of the methanol injection pressure and methanol substitution percentage (MSP) was also investigated for the DI_L configuration at 5 bar IMEP, revealing that the combustion process was relatively insensitive to the methanol injection pressure but was adversely affected by increasing the MSP. Both port and DI_L configurations produced lower greenhouse gas emissions than the pure Diesel reference case under various load conditions. However, only the methanol port injection configuration achieved ultra-low NOx and soot emissions at 12 bar IMEP.

Author's contribution: ZJ performed the experiments together with Dr. Benham, post-processed the data, and wrote the article. Prof. Denbratt gave support in experimental planning and paper writing.

# Appendix

## A. Heat Release Analysis

In Paper IV and V, the gross rate of heat release was calculated using a Matlab script based on Heywood [107]. The cylinder is considered to be a thermodynamically closed system in the heat release analysis. Based on the first law of thermodynamics, the energy conservation in the cylinder can be expressed as:

$$\delta Q = dU + \delta W \tag{A.1}$$

where $\delta Q$ is the heat transfer change of the cylinder, $dU$ is the internal energy change of the cylinder and $\delta W$ is the work transfer change from the piston. $\delta Q$ consists of two part: $\delta Q_{ch}$ is the heat transfer change to the cylinder and $\delta Q_{ht}$ is the heat transfer change from the cylinder ( $\delta Q$=$\delta Q_{ch}$-$\delta Q_{ht}$).

If it is assumed that the contents of the cylinder can be modeled as an ideal gas, the internal energy $U$ can be expessed as:

$$U = mc_v T \tag{A.2}$$

where $m$ is the mass in the cylinder, $c_v$ is the specific heat at constant volume and $T$ is the temperature.

If the mass in the cylinder $m$ is constant, the derivative of $U$ is:

$$\frac{dU}{dt} = mc_v \frac{dT}{dt} \tag{A.3}$$

From the ideal gas law:

$$pV = mRT \tag{A.4}$$

where $p$ is the cylinder pressure, $V$ is the volume of the combustion chamber and $R$ is the ideal gas constant, it follows that:

$$\frac{dp}{p} + \frac{dV}{V} = \frac{dT}{T} \tag{A.5}$$

Using Equation A.4 and A.5, Equation A.3 can be rewritten as:

$$\frac{dU}{dt} = \frac{c_v}{R}(p\frac{dV}{dt} + V\frac{dp}{dt}) \tag{A.6}$$

The constant pressure heat capacity ($c_p$) of the cylinder gas mixture is calculated using NIST polynomials. $c_v$ can be calculated as:

$$c_v = c_p - R \tag{A.7}$$

The work transfer change from the piston to gas can be calculated as:

$$\delta W = pdV \tag{A.8}$$

The heat transfer from the cylinder to walls has been estimated using the model proposed by Woschni.

$$\frac{dQ_{ht}}{dt} = hA(T - Twall) \tag{A.9}$$

where $A$ is the wall area. Woschni's correlation for the heat transfer coefficient can be expressed as:

$$h = 3.26 \cdot B^{-0.2} \cdot p^{0.8} \cdot T^{-0.55} \cdot w^{0.8} \tag{A.10}$$

where $B$ is the cylinder diameter, $p$ is the cylinder pressure, $T$ is the mean cylinder gas temperature and $w$ is the average cylinder gas velocity.

The rate of heat release expressed as a function of crank angle ($\theta$) was used for engine study. Hence, the gross rate of heat release can be expressed as:

$$\frac{dQ_{ch}}{d\theta} = p(1 + \frac{c_v}{R})\frac{dV}{d\theta} + V\frac{dp}{d\theta} + \frac{dQ_{ht}}{d\theta} \tag{A.11}$$

# B. Cumulative heat release

The accumulated heat release could be obtained by integrating the rate of heat release over crank angles. Three important combustion parameters could be derived from it: namely start of combustion, combustion phasing and combustion duration, respectively. As shown in Figure B.1, the start of combustion and combustion phasing are defined as the crank angle where 5% (CA05) and 50% (CA50) of the total heat are released, respectively. Combustion duration is defined as the crank angle between 10 and 90% of total heat release (CA90-CA10).

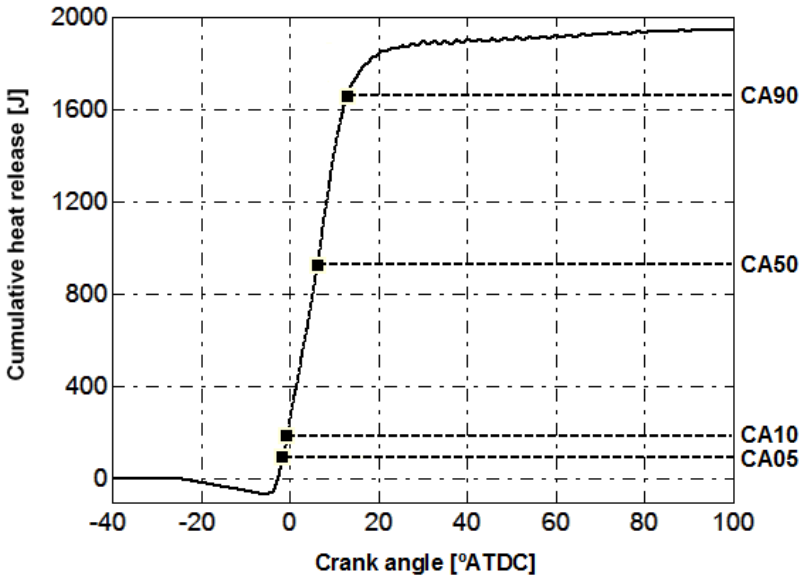


Figure B.1: Cumulative heat release with combustion timings when 5%, 10%, 50% and 90% of the total heat release

# References


[1] K. G. Hoyer, "Alternative fuels and sustainable mobility: is the future road paved by biofuels, electricity or hydrogen?" *International Journal of Alternative Propulsion*, vol. 1, no. 4, pp. 352–368, 2007.

[2] L. Wei, C. Yao, G. Han, and W. Pan, "Effects of methanol to Diesel ratio and Diesel injection timing on combustion, performance and emissions of a methanol port premixed diesel engine", *Energy*, vol. 95, pp. 223–232, 2016.

[3] C. Yao, C. S. Chunde, C. Cheng, and Y. Wang, "Reduction of smoke and $NO_x$ from Diesel engines using a Diesel/methanol compound combustion system", *Energy & Fuels*, vol. 21, no. 2, pp. 686–691, 2007.

[4] H. Tse, C. W. Leung, and C. S. Cheung, "Performance, emissions and soot properties from a Diesel-biodiesel-ethanol blend fueled engine", *Advances in Automobile Engineering*, pp. 1–7, 2016.

[5] "U.S. Energy Information Administration. International energy outlook 2017, https://www.eia.gov/outlooks/ieo/pdf/0484(2017).pdf", 2017.

[6] Q. Feng, J. Zhuang, and Z. Huang, "Influences of pilot injection and exhaust gas recirculation (EGR) on combustion and emissions in a HCCI-DI combustion engine", *Applied Thermal Engineering*, vol. 48, pp. 97–104, 2012.

[7] S. L. Kokjohn, R. M. Hanson, D. A. Splitter, J. Kaddatz, and R. D. Reitz, "Fuel reactivity controlled compression ignition (RCCI) combustion in light- and heavy-duty engines", SAE Paper No.2011-01-0357, 2011.

[8] C. Noehre, M. Andersson, B. Johansson, and A. Hultqvist, "Characterization of partially premixed combustion", SAE Paper No.2006-01-3412, 2006.

[9] G. A. Lechner, T. J. Jacobs, C. A. Chryssakis, D. N. Assanis, and R. N. Siewert, "Evaluation of a narrow spray cone angle, advanced injection timing strategy to achieve partially premixed compression ignition combustion in a diesel engine", SAE Paper No.2005-01-0167, 2005.

[10] I. Denbratt, "Method of controlling the process of combustion in an internal combustion engine, and engine with means for controlling the engine valves", Patent application No. WO0028197, Volvo Car Corp., 1999.

[11] L. Koopmans and I. Denbratt, "A four stroke camless engine, operated in homogeneous charge compression ignition mode with commercial gasoline", SAE Paper No.2001-01-3610, 2001.

[12] L. Koopmans, O. Roy, and I. Denbratt, "Direct gasoline injection in the negative valve overlap of a homogeneous charge compression ignition engine", SAE Paper No.2003-01-1854, 2003.

[13] T. Chen, H. Xie, W. Yu, L. Zhang, and H. Zhao, "Expanding the low load limit of HCCI combustion process using EIVO strategy in a 4VVAS gasoline engine", SAE Paper No.2012-01-1121, 2012.

[14] H. Yun, N. Wermuth, and P. Najt, "Development of robust gasoline HCCI idle operation using multiple injection and multiple ignition (MIMI) strategy", SAE Paper No.2009-01-0499, 2009.

[15] D. Dahl, M. Andersson, A. Berntsson, L. Koopmans, and I. Denbratt, "Reducing pressure fluctuations at high loads by means of charge stratification in HCCI combustion with negative valve overlap", SAE Paper No.2009-01-1785, 2009.

[16] D. Dahl and I. Denbratt, "HCCI/SCCI load limits and stoichiometric operation in a multicylinder naturally aspirated spark ignition engine operated on gasoline and e85", *International Journal of Engine Research*, vol. 12, no. 1, pp. 58–68, 2010.

[17] D. Dahl, M. Andersson, and I. Denbratt, "The role of charge stratification for reducing ringing in gasoline engine homogeneous charge compression ignition combustion investigated by optical imaging", *International Journal of Engine Research*, vol. 14, no. 5, pp. 525–536, 2013.

[18] F. Xu, Z. Wang, D. B. Yang, and J. X. Wang, "The role of charge stratification for reducing ringing in gasoline engine homogeneous

charge compression ignition combustion investigated by optical imaging", *Energy & Fuels*, vol. 23, pp. 2444–2452, 2009.

[19] C. N. Noehre, M. Andersson, B. Johansson, and A. Hultqvist, "Characterization of partially premixed combustion", SAE Paper No.2006-01-3412, 2006.

[20] S. Kimura, H. Ogawa, Y. Matsui, and Y. Enomoto, "An experimental analysis of low-temperature and premixed combustion for simultaneous reduction of $no_x$ and particulate emissions in direct injection diesel engines", *International Journal of Engine Research*, vol. 3, no. 4, pp. 249–259, 2002.

[21] M. Alriksson and I. Denbratt, "Low temperature combustion in a heavy duty Diesel engine using high levels of EGR", SAE Paper No.2006-01-0075, 2006.

[22] V. Manente, B. Johansson, P. Tunestal, and W. Cannella, "Effects of different type of gasoline fuels on heavy duty partially premixed combustion", *SAE Int. J. Engines*, vol. 2, no. 2, pp. 71–88, 2009.

[23] V. Manente, B. Johansson, P. Tunestal, W. Cannella, and C. Zoran, "An advanced internal combustion engine concept for low emissions and high efficiency from idle to max load using gasoline partially premixed combustion", SAE Paper No.2010-01-2198, 2010.

[24] M. C. Sellnau, J. Sinnamon, K. Hoyer, and H. Husted, "Effects of different type of gasoline fuels on heavy duty partially premixed combustion", *SAE Int. J. Engines*, vol. 5, pp. 300–314, 2012.

[25] M. Q. Shen, M. Tuner, and B. Johansson, "Close to stoichiometric partially premixed combustion - the benefit of ethanol in comparison to conventional fuels", SAE Paper No.2013-01-0277, 2013.

[26] K. Inagaki, T. Fuyuto, K. Nishikawa, and K. Nakakita, "Dual-fuel PCI combustion controlled by in-cylinder stratification of ignitability", SAE Paper No.2006-01-0028, 2006.

[27] D. Splitter, R. Hanson, S. Kokjohn, and R. Reitz, "Reactivity controlled compression ignition (RCCI) heavy-duty engine operation at mid- and high- loads with conventional and alternative fuels", SAE Paper No.2011-01-0363, 2011.

[28] A. Paykani, A. Kakaee, P. Rahnama, and R. D. Reitz, "Progress and recent trends in reactivity-controlled compression ignition engines",

*International Journal of Engine Research*, vol. 17, no. 5, pp. 481–524, 2016.

[29] R. D. Reitz and G. Duraisamy, "Review of high efficiency and clean reactivity controlled compression ignition (RCCI) combustion in internal combustion engines", *Progress in Energy and Combustion Science*, vol. 46, pp. 12–71, 2015.

[30] R. M. Hanson, S. L. Kokjohn, D. A. Splitter, and R. D. Reitz, "An experimental investigation of fuel reactivity controlled PCCI combustion in a heavy-duty engine", *SAE Int. J. Engines*, vol. 3, no. 1, pp. 700–716, 2010.

[31] S. Y. Ma, Z. Q. Zheng, H. F. Liu, Q. C. Zhang, and M. F. Yao, "Experimental investigation of the effects of diesel injection strategy on gasoline/diesel dual-fuel combustion", *Applied Energy*, vol. 109, pp. 202–212, 2013.

[32] C. Leermakers, B. Van den Berge, C. Luijten, L. Somers, L. de Goey, and B. Albrecht, "Gasoline-diesel dual fuel: Effect of injection timing and fuel balance", SAE Paper No.2011-01-2437, 2011.

[33] R. Hanson, S. Kokjohn, D. Splitter, and R. D. Reitz, "Fuel effects on reactivity controlled compression ignition (RCCI) combustion at low load", *SAE Int. J. Engines*, vol. 4, no. 1, pp. 394–411, 2011.

[34] D. Splitter, R. Hanson, S. Kokjohn, M. Wissink, and R. D. Reitz, "Injection effects in low load RCCI dual-fuel combustion", SAE Paper No.2011-24-0047, 2011.

[35] D. Splitter, M. Wissink, T. L. Hendricks, J. B. Ghandhi, and R. D. Reitz, "Comparison of RCCI, HCCI, and CDC operation from low to full load", THIESEL 2012 Conferences on Thermo- and Fluid Dynamic Processes in Direct Injection Engines, 2012.

[36] S. Molina, A. Garcia, J. M. Pastor, E. Belarte, and I. Balloul, "Operating range extension of RCCI combustion concept from low to full load in a heavy-duty engine", *Applied Energy*, vol. 143, pp. 211–227, 2015.

[37] R. Hanson and R. D. Reitz, "Transient RCCI operation in a light-duty multi-cylinder engine", *SAE Int. J. Engines*, vol. 6, no. 3, pp. 1694–1705, 2013.

[38] S. L. Kokjohn and R. D. Reitz, "Chemiluminescence and fuel PLIF imaging of reactivity controlled compression ignition (RCCI) combustion", ILASS Americas SAND2011-2009C, 2011.

[39] S. L. Kokjohn, M. P. B. Musculus, and R. D. Reitz, "Evaluating temperature and fuel stratification for heat-release rate control in a reactivity-controlled compression-ignition engine using optical diagnostics and chemical kinetics modeling", *Combustion and Flame*, vol. 162, pp. 2729–2742, 2015.

[40] Q. L. Tang, H. F. Liu, and M. F. Yao, "Simultaneous measurement of natural flame luminosity and emission spectra in a RCCI engine under different fuel stratification degrees", *SAE Int. J. Engines*, vol. 10, no. 3, pp. 1155–1162, 2017.

[41] G. Roberts, C. M. Rousselle, M. Musculus, M. Wissink, S. Curran, and E. Eagle, "RCCI combustion regime transitions in a single-cylinder optical engine and a multi-cylinder metal engine", SAE Int. J. Engines No. 2017-24-0088, 2017.

[42] S. L. Kokjohn, R. M. Hanson, D. A. Splitter, and R. D. Reitz, "Experiments and modeling of dual-fuel HCCI and PCCI combustion using in-cylinder fuel blending", *SAE Int. J. Engines*, vol. 2, no. 2, pp. 24–39, 2009.

[43] S. L. Kokjohn, R. M. Hanson, D. A. Splitter, and R. D. Reitz, "Fuel reactivity controlled compression ignition (RCCI): a pathway to controlled high-efficiency clean combustion", *International Journal of Engine Research*, vol. 12, no. 3, pp. 209–226, 2011.

[44] A. B. Dempsey and R. D. Reitz, "Fuel reactivity controlled compression ignition (RCCI): a pathway to controlled high-efficiency clean combustion", *SAE Int. J. Engines*, vol. 4, no. 2, pp. 2222–2239, 2011.

[45] J. H. Lim and R. D. Reitz, "High load (21 Bar IMEP) dual fuel RCCI combustion using dual direct injection", *Journal of Engineering for Gas Turbines and Power*, vol. 136, no. 10, p. Article number 101514, 2014.

[46] J. Campos-Fernandez, J. Arnal, J. Gomez, and M. Pilar Dorado, "A comparison of performance of higher alcohols/Diesel fuel blends in a Diesel engine", *Applied Energy*, vol. 95, pp. 267–275, 2012.

[47] Z. H. Huang, H. B. Lu, D. M. Jiang, K. Zeng, B. Liu, and J. Q. Zhang, "Combustion behaviors of a compression ignition engine fueled with

Diesel/methanol blends under various fuel delivery advance angles", *Bioresource Technology*, vol. 95, no. 3, pp. 331–341, 2004.

[48] R. L. Swamy, T. K. Chandrashekar, N. R. Banapurmath, and S. V. Khandal, "Impact of Diesel-butanol blends on performance and emissions of diesel engine", *Oil and Gas Research*, vol. 1, no. 1, pp. 1–7, 2004.

[49] T. K. Zhang, L. J. Nilsson, C. Bjorkholtz, K. Munch, and I. Denbratt, "Effect of using butanol and octanol isomers on engine performance of steady state and cold start ability in different types of Diesel engines", *Fuel*, vol. 184, pp. 708–717, 2016.

[50] C. Sayin, A. N. Ozsezen, and M. Canakci, "The influence of operating parameters on the performance and emissions of a di diesel engine using methanol-blended-Diesel fuel", *Fuel*, vol. 89, no. 7, pp. 1407–1414, 2010.

[51] S. K. Masimalai, "Influence of methanol induction on performance, emission and combustion behavior of a methanol-Diesel dual fuel engine", SAE Paper No.2014-01-1315, 2014.

[52] Q. Wang, L. Wei, W. Pan, and C. Yao, "Investigation of operating range in a methanol fumigated Diesel engine", *Fuel*, vol. 140, pp. 164–170, 2015.

[53] L. J. Wang, R. Z. Song, H. Zou, S. H. Liu, and L. B. Zhou, "Study on combustion characteristics of a methanol-Diesel dual-fuel compression ignition engine", *Proceedings of the Institution of Mechanical Engineers, Part D: Journal of Automobile Engineering*, vol. 222, no. 4, pp. 619–627, 2008.

[54] Z. Zhang, C. Cheung, and C. Yao, "Influence of fumigation methanol on the combustion and particulate emissions of a Diesel engine", *Fuel*, vol. 111, pp. 442–448, 2013.

[55] H. Wei, C. Yao, W. Pan, G. Han, Z. Dou, T. Wu, M. Liu, B. Wang, J. Gao, C. Chen, and J. Shi, "Experimental investigations of the effects of pilot injection on combustion and gaseous emission characteristics of Diesel/methanol dual fuel engine", *Fuel*, vol. 188, pp. 427–441, 2017.

[56] F. Zhang, X. Zhang, S. Shuai, J. Xiao, and J. Wang, "Unregulated emissions and combustion characteristics of low-content methanol-

gasoline blended fuels", *Energy & Fuels*, vol. 24, no. 2, pp. 1283–1292, 2010.

[57] F. Zhang, X. Zhang, S. Shuai, J. Xiao, and J. Wang, "Regulated and unregulated emissions from a Diesel engine fueled with biodiesel and biodiesel blended with methanol", *Atmospheric Environment*, vol. 43, no. 32, pp. 4865–4872, 2009.

[58] A. B. Dempsey, N. R. Walker, and R. D. Reitz, "Effect of piston bowl geometry on dual fuel reactivity controlled compression ignition (RCCI) in a light-duty engine operated with gasoline/Diesel and methanol/Diesel", *SAE Int. J. Engines*, vol. 6, no. 1, pp. 78–100, 2013.

[59] A. B. Dempsey, N. R. Walker, and R. D. Reitz, "Effect of cetane improvers on gasoline, ethanol, and methanol reactivity and the implications for RCCI combustion", *SAE Int. J. Fuels Lubr.*, vol. 6, no. 1, pp. 170–187, 2013.

[60] Y. Li, M. Jia, Y. Liu, and M. Xie, "Numerical study on the combustion and emission characteristics of a methanol/Diesel reactivity controlled compression ignition (RCCI) engine", *Applied Energy*, vol. 106, pp. 184–197, 2013.

[61] Y. Li, M. Jia, Y. Chang, Y. Liu, M. Xie, and T. Wang, "Parametric study and optimization of a RCCI (reactivity controlled compression ignition) engine fueled with methanol and Diesel", *Energy*, vol. 65, pp. 319–332, 2014.

[62] Y. Li, M. Jia, Y. Chang, M. Xie, and R. D. Reitz, "Towards a comprehensive understanding of the influence of fuel properties on the combustion characteristics of a RCCI (reactivity controlled compression ignition) engine", *Energy*, vol. 99, pp. 69–82, 2016.

[63] X. Zou, H. Wang, Z. Zheng, R. D. Reitz, and M. Yao, "Numerical study of the RCCI combustion processes fuelled with methanol, ethanol, n-butanol and Diesel", SAE Paper No.2016-01-0777, 2016.

[64] T. L. Ullman, C. T. Hare, and T. M. Baines, "Emission from direct-injected heavy-duty methanol-fueled engines (one dual-injection and one spark-ignited) and a comparable Diesel engine", SAE Paper No.820966, 1982.

[65] J. A. LuRusso and H. A. Cikanek, "Direct injection ignition assisted alcohol engine", SAE Paper No.880495, 1988.

[66] M. L. Wissink, J. H. Lim, D. A. Splitter, R. M. Hanson, and R. D. Reitz, "Investigation of injection strategies to improve high efficiency RCCI combustion with diesel and gasoline direct injection", *Proceedings of ASME Internal Combustion Engine Division Fall Technical Conference ICEF2012-92107* , 2012.

[67] G. A. Karim, "A review of combustion process in the dual fuel engine - the gas Diesel engine", *Energy Combustion Science*, vol. 6, pp. 277–285, 1980.

[68] G. A. Karim, "The dual fuel engine of the compression ignition type - prospects, problems and solutions - A review", SAE Paper No.831073, 1983.

[69] B. B. Sahoo, N. Sahoo, and U. K. Saha, "Effect of engine parameters and type of gaseous fuel on the performance of dual-fuel gas Diesel engines - A critical review", *Renewable and Sustainable Energy Reviews*, vol. 6, pp. 277–285, 1980.

[70] T. Korakianitis, R. M. Namasivayam, and R. J. Crookes, "Natural-gas fueled spark-ignition (SI) and compression-ignition (CI) engine performance and emissions", *Progress in Energy and Combustion Science*, vol. 37, pp. 89–112, 2011.

[71] G. A. Karim, "Combustion in gas fueled compression: ignition engines of the dual fuel type", *International Engineering for Gas Turbines and Power*, vol. 125, pp. 827–836, 2003.

[72] U. Azimov, E. Tomita, N. Kawahara, and Y. Harada, "Premixed mixture ignition in the end-gas region (PREMIER) combustion in a natural gas dual-fuel engine: operating range and exhaust emissions", *International Journal of Engine Research*, vol. 12, no. 5, pp. 484–497, 2011.

[73] G. H. Abd Alla, H. A. Soliman, O. Badr, and M. F. Abd Rabbo, "Effect of pilot fuel quantity on the performance of a dual fuel engine", SAE Paper No.1999-01-3597, 1999.

[74] Z. Q. Lin and W. H. Su, "A study on the determination of the amount of pilot injection and rich and lean boundaries of the premixed CNG/air mixture for a CNG/Diesel dual-fuel engine", SAE Paper No.2003-01-0765, 2003.

[75] S. R. Krishnan, K. K. Srinivasan, S. Singh, S. R. Bell, K. C. Midkiff, W. Gong, S. B. Fiveland, and M. Willi, "Combustion and exhaust

emission characteristics of a dual fuel compression ignition engine operated with pilot Diesel fuel and natural gas", *Journal of Engineering for Gas Turbines and Power*, vol. 126, pp. 665–671, 2004.

[76] T. Tagai, M. Ishida, and H. Ueki, "Effects of equivalence ratio and temperature of CNG premixture on knock limit in a dual fueled Diesel engine", SAE Paper No.2003-01-1934, 2003.

[77] T. Ishiyama, J. Kang, and Y. Ozawa, "Improvement of performance and reduction of exhaust emissions by pilot-fuel-injection control in a lean-burning natural-gas dual-fuel engine", SAE Paper No.2011-01-1963, 2011.

[78] M. M. Abdelaal and A. H. Hegab, "Combustion and emission characteristics of a natural gas-fueled Diesel engine with EGR", *Energy Conversion and Management*, vol. 64, pp. 2971–2987, 2012.

[79] M. Ishida, T. Tagai, and H. Ueki, "Effect of EGR and preheating on natural gas combustion assisted with gas-oil in a Diesel engine", *JSME International Journal*, vol. 46, no. 1, pp. 124–130, 2003.

[80] E. Tomita, N. Kawahara, Z. Piao, and R. Yamaguchi, "Effects of EGR and early injection of Diesel fuel on combustion characteristics and exhaust emissions in a methane dual fuel engine", SAE Paper No.2002-01-2723, 2002.

[81] Z. Stelmasiak, "The impact of gas-air composition on combustion parameters of dual-fuel engines fed CNG", SAE Paper No.2002-01-2235, 2002.

[82] J. J. Zheng, J. H. Wang, and Z. H. Huang, "Effect of the compression ratio on the performance and combustion of a natural-gas direct-injection engine", *Proc. IMechE*, vol. 223, pp. 85–98, 2009.

[83] R. G. Papagiannakis, D. T. Hountalas, C. D. Rakopoulos, and D. C. Rakopoulos, "Combustion and performance characteristics of a DI Diesel engine operating from low to high natural gas supplement ratios at various operating conditions", SAE Paper No.2008-01-1392, 2008.

[84] R. G. Papagiannakis and D. T. Hountalas, "Combustion and exhaust emission characteristics of a dual fuel compression ignition engine operated with pilot Diesel fuel and natural gas", *Energy Conversion and Management*, vol. 45, pp. 2971–2987, 2004.

[85] S. R. Krishnan, Y. M. Biruduganti, S. R. Bell, and K. C. Midkiff, "Performance and heat release analysis of a pilot-ignited natural gas engine", *International Journal of Engine Research*, vol. 3, no. 3, pp. 171–184, 2002.

[86] S. R. Krishnan, Y. M. Biruduganti, S. R. Bell, and K. C. Midkiff, "Assessment of combustion in natural gas fueled compression ignition engines with DME and RME pilot ignition", *Proceedings of the Institution of Mechanical Engineering International Journal of Engine Research*, vol. 10, no. 3, pp. 165–174, 2009.

[87] A. E. Felt and W. A. Steele, "Combustion control in dual-fuel engines", SAE Paper No.620555, 1962.

[88] G. A. Karim, S. R. Klat, and N. P. W. Moore, "Knock in dual-fuel engines", *Proceedings of the Institution of Mechanical Engineering*, vol. 181, no. 1, pp. 453–466, 1996.

[89] N. N. Mustafi and R. R. Raine, "A study of the emissions of a dual fuel engine operating with alternative gaseous fuels", SAE Paper No.2008-01-1394, 2008.

[90] I. Glassman and R. A. Yetter, *Combustion*. Elsevier, 2008.

[91] D. E. Nieman, A. B. Dempsey, and R. D. Reitz, "Heavy-duty RCCI operation using natural gas and Diesel", *SAE Int. J. Engines*, vol. 5, no. 2, pp. 270–285, 2012.

[92] P. Zoldak, A. Sobiesiak, M. Bergin, and D. D. Wickman, "Computational study of reactivity controlled compression ignition (RCCI) combustion in a heavy-duty Diesel engine using natural gas", SAE Paper No.2014-01-1321, 2014.

[93] N. Ryan Walker, M. L. Wissink, D. A. DelVescovo, and R. D. Reitz, "Natural gas for high load dual-fuel reactivity controlled compression ignition (RCCI) in heavy-duty engines", *Proceedings of ASME 2014 Internal Combustion Engine Division Fall Technical Conference ICEF2014-5620*, 2014.

[94] S. L. Kokjohn, "Experimental demonstration of RCCI in heavy-duty engines using Diesel and natural gas", SAE Paper No.2014-01-1318, 2014.

[95] M. Dahodwala, S. Joshi, E. Koehler, M. Franke, and D. Tomazic, "Experimental and computational analysis of Diesel-natural gas RCCI

combustion in heavy-duty engines", SAE Paper No.2015-01-0849, 2015.

[96] J. Li, W. M. Yang, H. An, D. Z. Zhou, and M. Kraft, "Application of dynamic $\phi - T$ map: Analysis on a natural gas/Diesel fueled RCCI engine", *Journal of Engineering of Gas Turbines and Power*, vol. 138, no. 9, pp. 092 803–1–10, 2016.

[97] J. Li, W. M. Yang, H. An, and D. Z. Zhou, "Soot and NO emissions control in a natural gas/Diesel fuelled RCCI engine by $\phi - T$ map analysis", *Combustion Theory and Modelling*, vol. 21, no. 2, pp. 309–328, 2016.

[98] B. D. Hsu, *Practical diesel-engine combustion analysis*. SAE International, 2002.

[99] J. F. Wakenell, G. B. O'Neal, and Q. A. Baker, "High-pressure late cycle direct injection of natural gas in a rail medium speed diesel engine", SAE Paper No.872041, 1987.

[100] A. Boretti, P. Lappas, B. Zhang, and S. K. Mazlan, "CNG fueling strategies for commercial vehicles engines - A literature review", SAE Paper No.2013-01-2812, 2013.

[101] B. D. Hsu, G. L. Confer, and R. E. McDowell, "The "H-Process" dual fuel diesel engine", *Natural Gas and Alternative Fuels for Engines*, vol. ICE24, pp. 25–30, 1995.

[102] G. McTaggart-Cowan, K. Mann, J. Huang, A. Singh, B. Patychuk, Z. X. Zheng, and S. Munshi, "Direct injection of natural gas at up to 600 bar in a pilot-ignited heavy-duty engine", *SAE Int. J. Engines*, vol. 8, no. 3, pp. 981–996, 2015.

[103] C. A. Laforet, B. S. Brown, S. N. Rogak, and S. R. Munshi, "Compression ignition of directly injected natural gas with entrained diesel", *International Journal of Engine Research*, vol. 11, no. 3, pp. 207–218, 2010.

[104] K. B. Hodgins, P. G. Hill, P. Ouellette, and P. Hung, "Directly injected natural gas fueling of diesel engines", SAE Paper No.961671, 1996.

[105] B. D. Hsu, "Method and apparatus for introducing fuel into a duel fuel system using the H-combustion process", U.S. Patent 5365902, 1994.

[106] J. Kubesh and S. R. King, "Effect of gas composition on octane number of natural gas fuels", SAE Paper No.922359, 1992.

[107] J. B. Heywood, *Internal combustion engine fundamentals*. McGraw-Hill, New York, 1988.

[108] V. I. Golovitchev, N. Nordin, R. Jarnicki, and J. Chomiak, "3D Diesel spray simulation using a new detailed chemistry turbulent combustion model", SAE Paper No.2000-01-1891, 2000.

[109] V. I. Golovitchev, K. Atarashiya, and S. Yamada, "Towards universal EDC-based combustion model for compression ignited engine simulations", SAE Paper No.2003-01-1849, 2003.

[110] A. Imren, V. I. Golovitchev, C. Sorusbay, and G. Valentino, "The full cycle HD diesel engine simulations using KIVA-4 code", SAE Paper No.2010-01-2234, 2010.

[111] A. N. Lipatnikov and J. Chomiak, "Turbulent flame speed and thickness: phenomenology, evaluation, and application in multi-dimensional simulations", *Progress in Energy and Combustion Science*, vol. 28, pp. 1–74, 2002.

[112] T. Joelsson, R. Yu, and X. S. Bai, "Large eddy simulation of turbulent combustion in a spark assisted homogeneous charge compression ignition engine", $7^{th}$ Mediterranean Combustion Symposium, Cagliari, Italy, 2011.

[113] R. J. Kee, F. M. Rupley, and J. A. Miller, "Chemkin II: A fortran chemical kinetics package for the analysis of gas phase chemical kinetics", Sandia report SAND89-8009B •UC-706, 1992.

[114] G. Borque, D. Healy, H. Curran, C. Zinner, D. Kalitan, J. de Vries, A. C., and E. Petersen, "Ignition and flame speed kinetics of two natural gas blends with high levels of heavier hydrocarbons", *Proc. ASME. Turbo Expo: Power for Land, Sea, and Air*, vol. 3, pp. 1051–1066, 2008.

[115] S. L. Kokjohn, "Reactivity controlled compression ignition (RCCI) combustion", Ph.D. thesis, University of Wisconsin-Madison, 2012.

[116] R. G. Papagiannakis and D. T. Hountalas, "Experimental investigation concerning the effect of natural gas percentage on performance and emissions of a DI dual fuel diesel engine", *Applied Thermal Engineering*, vol. 23, pp. 353–365, 2003.